AD-A069 842 TEXAS UNIV AT AUSTIN BIO-MEDICAL ENGINEERING RESEARCH LAB F/G 6/18
MEASUREMENTS IN THE LASER IRRADIATED EYE.(U)
NOV 78 A J WELCH, L D FORSTER AFOSR-77-3314

UNCLASSIFIED AFOSR-TR-79-0672 NL

1 OF 1
AD
A069842

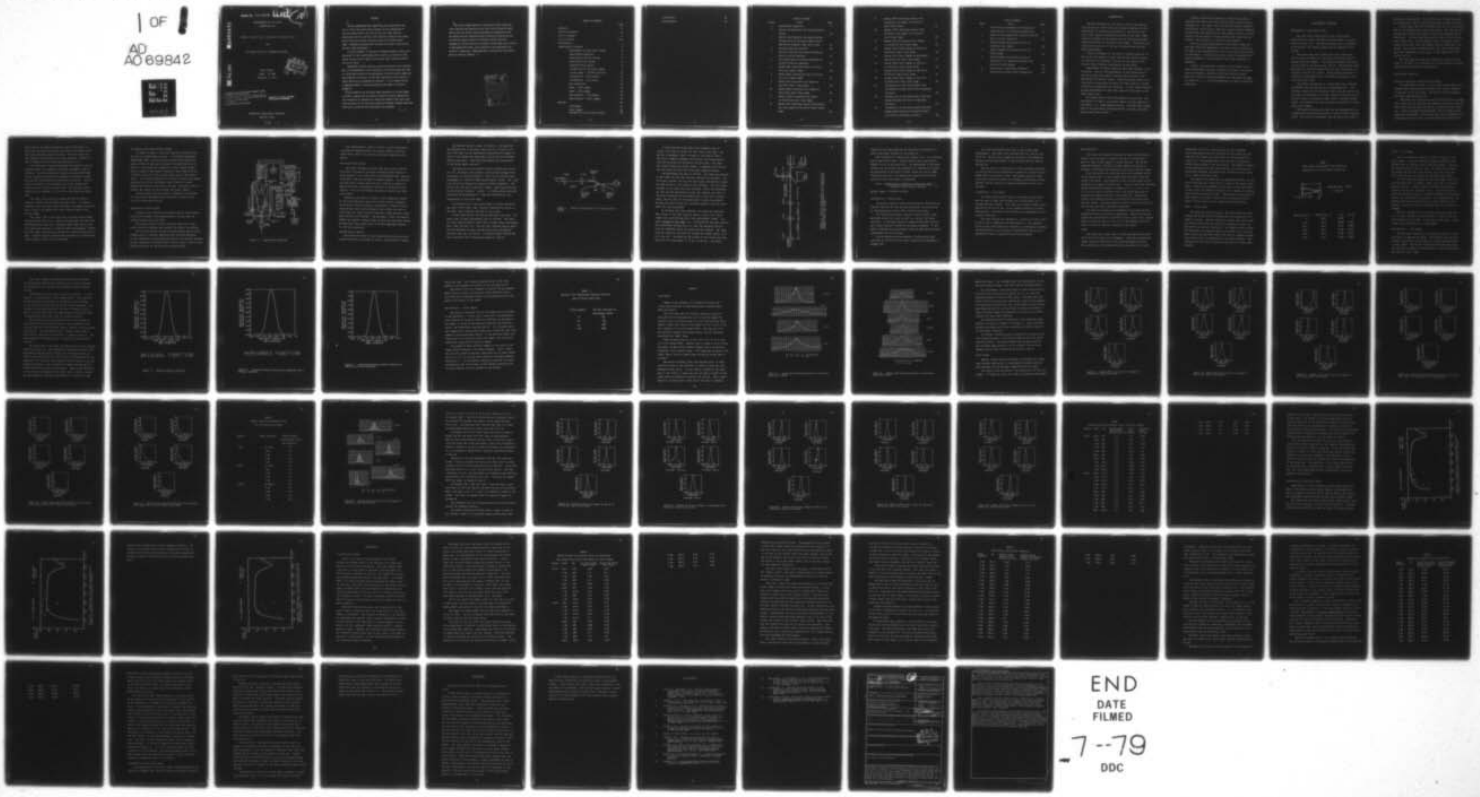

END
DATE
FILMED
7-79
DDC

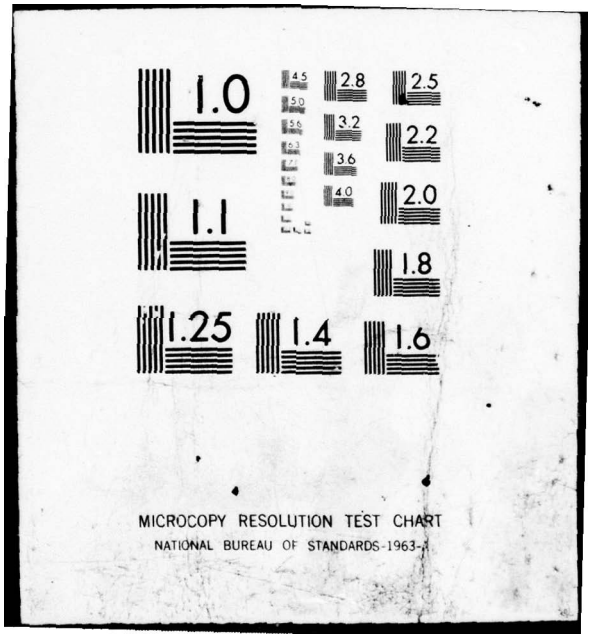
1.0
1.1
1.25
1.4
1.6
1.8
2.0
2.2
2.5
2.8
3.2
3.6
4.0
4.5
5.0
5.6
6.3
MICROCOPY RESOLUTION TEST CHART
NATIONAL BUREAU OF STANDARDS-1963-A

MEASUREMENTS IN THE LASER IRRADIATED EYE

Ashley J. Welch, Ph.D. and Larry D. Forster, Ph.D.

FOR

AIR FORCE OFFICE OF SPONSORED RESEARCH

FINAL REPORT

AFOSR - 77-3374

November 15, 1978

BIOMEDICAL ENGINEERING LABORATORY

AUSTIN, TEXAS

ABSTRACT

The work ~~described in this report~~ involves the fabrication and use of a small fiber optic probe to measure (1) the transmission of the ocular media which is the ratio of the total light intensity reaching the retina to the total light intensity incident on the cornea, and (2) the cross-sectional intensity profile of a minimally small image. Information concerning the resolution of the eye is derived from the small image measurements.

Critical parameters in the study of damage mechanisms in the eye are the amount of light reaching the retinal tissues as a function of wavelength, and the size and shape of the relative light intensity distribution on the retina.

Measurements of these quantities have been reported in the literature. Most of the measurements of the transmission of the ocular media were made on excised eyes and most of the measurements of minimal retinal images were made either on excised eyes, or were made indirectly on intact eyes by a fundus reflective or psychophysical technique. In this research direct, in vivo measurements of these two quantities were made in the rhesus monkey eye.

The transmission of the ocular media, measured on a limited number of animals, compares well with some of the best previously reported data. The transmission was measured via a 600 micron diameter fiber optic probe which collected all the light from a 200 micron diameter irrading laser beam. Three lasers, providing seven wavelengths, were employed.

The minimal images measured in the monkey eye were larger than values reported from subjective acuity tests or by diffraction theory. Some of this poor quality could be attributed to experimental error, but perhaps the most significant factor affecting eye quality was the fact that the neural controls for blinking, tearing, and micro-accomodation, which aid the eye in forming a retinal image, were inactive in the anesthetized animal. If eye quality in the experimental preparation is indeed poor, other experiments involving fine visual detail would be similarly affected.

TABLE OF CONTENTS

	Page
Abstract	ii
Table of Contents	iv
List of Figures	vi
List of Tables	viii
Introduction	1
Experimental Procedure	3
Development of Fiber Optic Probe	3
Experimental Apparatus	4
Experimental Control System	6
Data Acquisition System	8
Scanning Mirror System	8
Transmission of the Ocular Media	9
Minimal Image - Transfer Function	13
Illumination - Point Source	13
Illumination - Line Source	14
Eye Preparation	15
Scans - Point Image	16
Scans - Line Images	18
Data Analysis - Line Images	18
Data Analysis - Point Images	23
Results	25
Line Images	25
Point Images	28
Transmission of the Ocular Media	45

Conclusions 65

Bibliography 67

LIST OF FIGURES

Figure	Title	Page
1	Experimental Apparatus	7
2	Optical Configuration for Scanning Mirror System	10
3	Optical Configuration for Measuring the Transmission of the Ocular Media with a 600 Micron Diameter Fiber Optic Probe	12
4	Original Gaussian Function	20
5	Gaussian Function Pertrubed by Sampling with a Circular Aperture	21
6	Perturbed Gaussian Function Restored by Inverse Filtering Technique	22
7	Monkey 9877 Misfocused Scans at Corrective Lens Powers Shown	26
8	Monkey 92077 Misfocused Scans at Corrective Lens Powers Shown	27
9	Monkey 9877 Corrected Line Images at Artifical Pupil Sizes Shown	29
10	Monkey 92077 Corrected Line Images at Artificial Pupil Sizes Shown	30
11	Monkey 121677 Corrected Line Images at Artificial Pupil Sizes Shown	31
12	Monkey 9877 Amplitude Spectra from Corrected Line Images at Artificial Pupil Sizes Shown	32

13	Monkey 92077 Amplitude Spectra from Corrected Line Images at Artificial Pupil Sizes Shown	33
14	Monkey 121677 Amplitude Spectra from Corrected Line Images at Artificial Pupil Sizes Shown	34
15	Monkey 10477 Misfocused Point Images at Corrective Lens Power Shown	36
16	Monkey 72177 Point Images at 630 nm at Artificial Pupil Sizes Shown	38
17	Monkey 72177 Point Images at Wavelength and Artificial Pupil Sizes Shown	39
18	Monkey 10477 Point Images at 455.5 nm at Artificial Pupil Sizes Shown	40
19	Monkey 10477 Point Images at 488 nm at Artificial Pupil Sizes Shown	41
20	Monkey 10477 Point Images at 514.5 nm at Artificial Pupil Sizes Shown	42
21	Transmission of the Ocular Media from Two Rabbits Plotted with Curve of Geeraets and Berry	46
22	Transmission of the Ocular Media from One Monkey Plotted with Curve of Geeraets and Berry	47
23	Transmission of the Ocular Media from One Monkey whose Cornea Had Clouded Plotted with Curve of Geeraets and Berry	49

LIST OF TABLES

Table	Title	Page
1	Focal Plane Displacement with Respect to Focusing Error in the Rhesus Monkey Eye	17
2	Spread of Two Dimensional Gaussian Profiles Due to Finite Probe Size	24
3	Widths Between Half-Height Points for Corrected Line Images	35
4	Widths Between Half-Height Points for Point Images	43
5	Widths Between Half-Height Points of Equivalent Line Images Calculated from Widths of Point Images	52
6	Diffraction Limited Spot Diameters	56
7	Diffraction Limited Cutoff Frequencies	60

INTRODUCTION

The work described in this report involves the fabrication and use of a small fiber optic probe to measure (1) the transmission of the ocular media which is the ratio of the total light intensity reaching the retina to the total light intensity incident on the cornea, and (2) the cross-sectional intensity profile of a minimally small image. Information concerning the resolution of the eye is derived from the small image measurements.

Critical parameters in the study of damage mechanisms in the eye are the amount of light reaching the retinal tissues as a function of wavelength, and the size and shape of the relative light intensity distribution on the retina.

Measurements of these quantities have been reported in the literature. Most of the measurements of the transmission of the ocular media were made on excised eyes and most of the measurements of minimal retinal images were made either on excised eyes, or were made indirectly on intact eyes by a fundus reflective or psychophysical technique. In this research, direct, in vivo measurements of these two quantities were made in the rhesus monkey eye.

Two factors which affect the quality of vision are: the attenuation of light in pre-retinal media, and the fidelity of the object - to - image mapping fuction. The fiber optic probe, used in the experiments discussed herein, provides some information about these factors.

Studies concerning the damage to retinal tissue due to radiation from lasers and other intense light sources require knowledge of: the shape, size, and relative spatial intensity distribution in the retinal image for a given corneal intensity distribution; the absorption of light energy in specific ocular tissues; and the amount of light reaching the retina (and absorbed in the tissues) as a function of wavelength.

Previous *in vivo* measurements of the retinal image have been made using the temperature rise due to direct absorption of light of microthermocouples, but a fiber optic probe affords two advantages: increased sensitivity, and the separation of tissue temperature rise information from light intensity information.

Finally, the techniques outlined in this report allow direct measurements *in vivo*, although the animals are anesthetized and otherwise altered by drugs and surgical trauma. Most other retinal image measurements have been made *in vitro* or indirectly, i.e., using psychophysical or fundus reflective techniques.

EXPERIMENTAL PROCEDURE

Development of Fiber Optic Probe

The fiber optic probes used in this research were either glass or quartz rods which had been drawn in a probe puller to small tips. The smallest probes had tip diameters of 10 microns; the largest probes had tip diameters of 40 microns.

The probes were vapor coated with a thin reflective coat of silver by means of a rotating probe holder within a vacuum deposition chamber. The coating prevented light entering the probe at any point except the tip. Approximately 2000 Angstroms of silver were deposited while the probes were continuously rotating in a holder. Approximately one micron of copper was electrodeposited on the probes afterwards to protect the silver films.

The probes were mounted in a probe mount that contained a Hamamatsu R761 photomultiplier tube photodetector. This detector, chosen for its convenient small size and sensitivity. Less than one microwatt of incident corneal irradiation was required to give an acceptable signal from a 10 micron diameter probe. This detector was used to measure the profiles of minimally small images.

The coupling between the probe and the photodetector was accomplished using Dow Corning 200, a viscous optical coupling fluid. The fluid was continuous from the end of the probe to

the face of the detector. Use of this fluid allowed the probes to be relatively short, a definite advantage in probe fabrication.

A large probe (600 micron diameter) was used for the measurement of the transmission of the ocular media. The probe was fabricated from a three inch length of 600 micron diameter quartz fiber optic. The ends were broken nearly flat by first scoring with a small file. On the detecting end of the probe a small amount of Torr-Seal resin was placed, and was ground flat after curing. This formed a diffusing disk; the sides of the probe were then coated with silver epoxy, so that light could enter only at the tip.

The large aperture probe was intended to collect all the light in the beam, as is described in the Experimental Procedure: Transmission of the Ocular Media section.

Experimental Apparatus

Surgical Preparation and Animal Positioning

The experimental animal, a 4 to 8 pound rhesus monkey, was tranquilized, anesthetized and prepared for surgical exposure of the back of the left globe. The details of this procedure have been reported earlier (8).

The animal was restrained via ear and bite bars on a stereotaxic stand, and the left eye was sutured into place so that the nodal point was very near the center of rotation of the stereotax. Using a Narishge micromanipulator and an Olympus stereo dissecting microscope, a drill probe made from a tungsten microelectrode and driven with a Cavitron ultrasonic dental drill,

was placed at the desired insertion site on the sclera. A small hole was made by carefully pulsing the ultrasonic drill and slowly advancing the drill probe. The drill probe was then removed and the fiber optic probe inserted. Details of this procedure have also been reported earlier (1).

The stereotaxic stand was equipped with Superior Electric stepping motors for automatic rotational movement in two directions. Position transducers (Hewlett-Packard 24DCDT-1000 linear variable differential transformers) provided a signal for precise, high-resolution indication of position. The horizontal resolution of the stereotax was 25 arc seconds (2.3 microns on the retina) per motor step; the vertical resolution was 16 arc seconds (1.5 microns on the retina) per motor step.

The fiber optic probe was scanned through the retinal image by rotating the eye about its nodal point. In some experiments, this was done in two directions, horizontal and vertical, so that a two-dimensional raster scan was made of the retinal image.

The lasers used in this work were a Spectra Physics Model 166 4W CW argon ion laser, a Spectra Physics Model 135 dye laser with Rhodamine 6G dye, and a Chromatix Model 1000 Nd:YAG laser. The lasers were mounted on a granite table approximately 3 meters from the table containing the stereotaxic stand and other equipment. Variable exposure duration was provided by a Vincent Associates shutter placed in the laser beam.

Irradiation and Fundus Viewing System

As shown in Figure 1, the laser beam was reflected into the eye via a 50/50 beam splitter. A calibrated radiometer (EG&G Model 580), received the beam transmitted through the beam splitter and was used to measure the power during irradiation. The fundus was viewed with a Zeiss fundus camera. Direct viewing of the fundus allowed the laser beam to be positioned at specific sites in the retina such as the macula lutea. This viewing technique also aided location of the probe insertion site since the fundus camera light was visible through the sclera on the back of the eye. The probe, once inserted, was usually visible through the fundus camera.

Various lenses and other optical components as required by a particular experiment were mounted on an optical rail in front of the beam splitter.

Experimental Control System

A Devices Ltd. Digitimer provided the master timing pulses by which the shutter, the stepping motors, and the data recording process were controlled.

The shutter control circuit received "open" and "close" pulses from the Digitimer and operated the shutter accordingly.

The 2-D scan control circuit received shutter pulses, motor stepping pulses, and data sampling pulses from the Digitimer. It then delivered the appropriate horizontal and vertical stepping pulses, generated a horizontal motor reverse signal, and also generated two pulses for selecting and recording data.

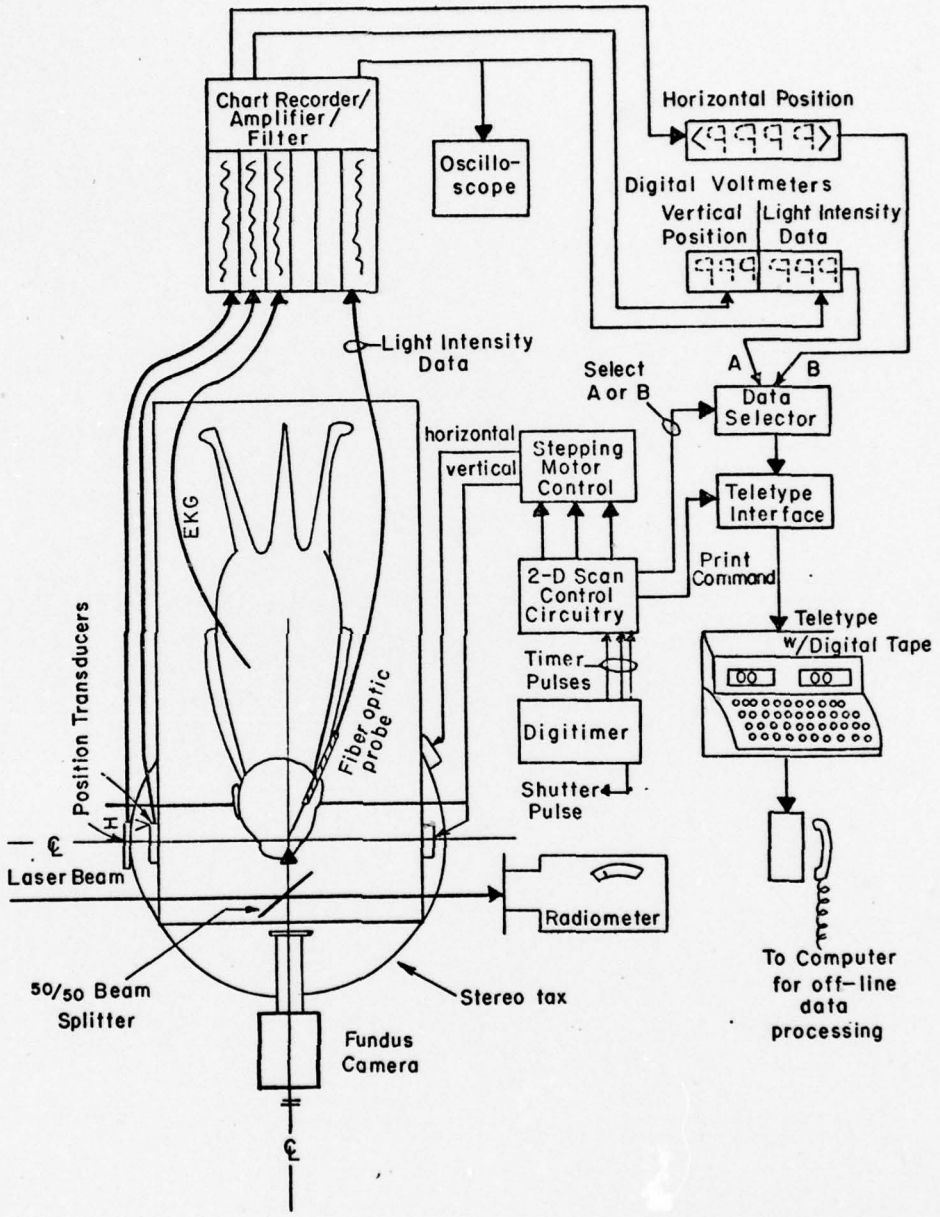

Figure 1. Experimental Apparatus.

The stepping motor control circuits, one for each motor, received the stepping pulses and reverse signals and translated these signals into the driver current required by the motors.

Data Acquisition System

The signal voltages from the fiber optic probe, and the horizontal and vertical position transducers were routed to three channels of an eight channel Clevite/Brush chart recorder. The animal's EKG was recorded on another channel. The position and fiber optic signals were low pass filtered to remove unwanted noise due to mechanical vibration or electrical interference. Also, an oscilloscope was used to monitor the fiber optic signal.

Referring once again to Figure 1, the respective outputs of the Brush amplifiers were fed to three digital voltmeters. The outputs of these voltmeters, which were in digital binary-coded-decimal form, were arranged so that either vertical position data and light intensity data were routed through a teletype interface and recorded. The teletype, a Texas Instruments 733ASR, has digital cassette tapes on which the data were stored. The data were later played back to the CDC 6600/6400 computer for off-line processing.

Scanning Mirror System

The speed with which the two dimensional raster scan could be made was greatly increased by using a scanning mirror system.

The optical system is shown in Figure 2. The beam size was adjusted with a telescope consisting of a 15 and a 5 cm lens; the beam size was determined by measuring the number of mirror steps between the beam peaks occuring at the different detector apertures. (See Probe Development and Transmission of the Ocular Media sections.)

The scanning mirrors (General Scanning AX200) were driven in a 20 x 20 point raster pattern by the analog voltages from two digital to analog converters. The D to A converters were programmed via a Motorola 6800 microprocessor system. The step size was easily adjusted by changing program parameters. The mirror step rate was 10 steps per second; data acquisition was via the Digital Voltmeter - Serdex - TI 733ASR system described previously which operated at a 1200 baud transmission rate.

Transmission of the Ocular Media

The transmission of the ocular media is herein defined as the ratio of the total light intensity reaching the retina to the total light intensity incident on the cornea.

A laser beam smaller than the dilated pupil was used. The lasers used in these measurements were as follows: The argon ion laser (Spectra-Physics Nidek 166) provided three wavelengths; 455.5, 488, and 514.5 nm. The dye laser (Spectra-Physics Model 135 with Rhodamine 6G dye) provided three more wavelengths; nominally 560, 590, and 630 nm. A Chromatix Model 1000 Nd:YAG laser provided a near infrared wavelength of 1060 nm.

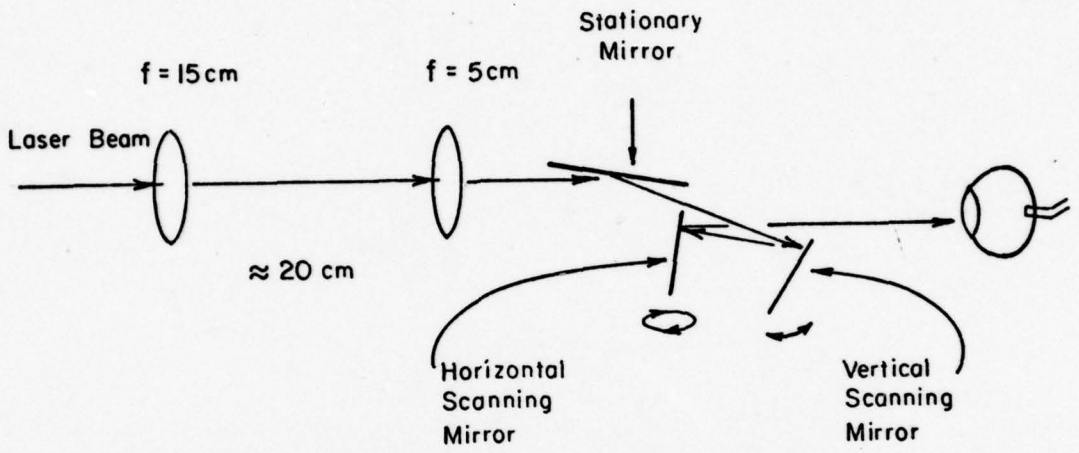

Figure 2 . Optical Configuration for Scanning Mirror System.

A large aperture probe (600 micron diameter) was inserted in the eye to collect all the light in the beam. The optical arrangement, shown in Figure 3, was used to form a 200 micron diameter (between $1/e^2$ points), collimated beam inside the eye which was directed on to the probe. The image was viewed through the fundus camera; it appeared to be smaller than the probe tip when the lenses were properly focused.

The measurement was made as follows. The image was centered on the probe tip such that the peak response was obtained. This value was recorded, and also the laser power transmitted through the beam splitter (see Figure 3) was recorded. The total power incident to the lenses was also recorded. After the experiment was over and the experimental animal was removed, the ratio of the power reflected off the beamsplitter to the total incident power, and the ratio of reflected power to power transmitted through the beam splitter was carefully measured with the radiometer for each wavelength.

To calibrate the probe response, its output was measured when placed in the same system as before, with a 2 cm. focal length lens replacing ghe eye of the experimental animal. The power <u>incident on the probe</u> (i.e., reflected off the beam splitter and transmitted through the 2 cm. lens) was measured directly with the radiometer after the probe had been removed. The image could be viewed on the probe tip through the fundus camera, just as in the eye. The probe was maintained at very nearly the same angle for this measurement as it was in the eye. The output

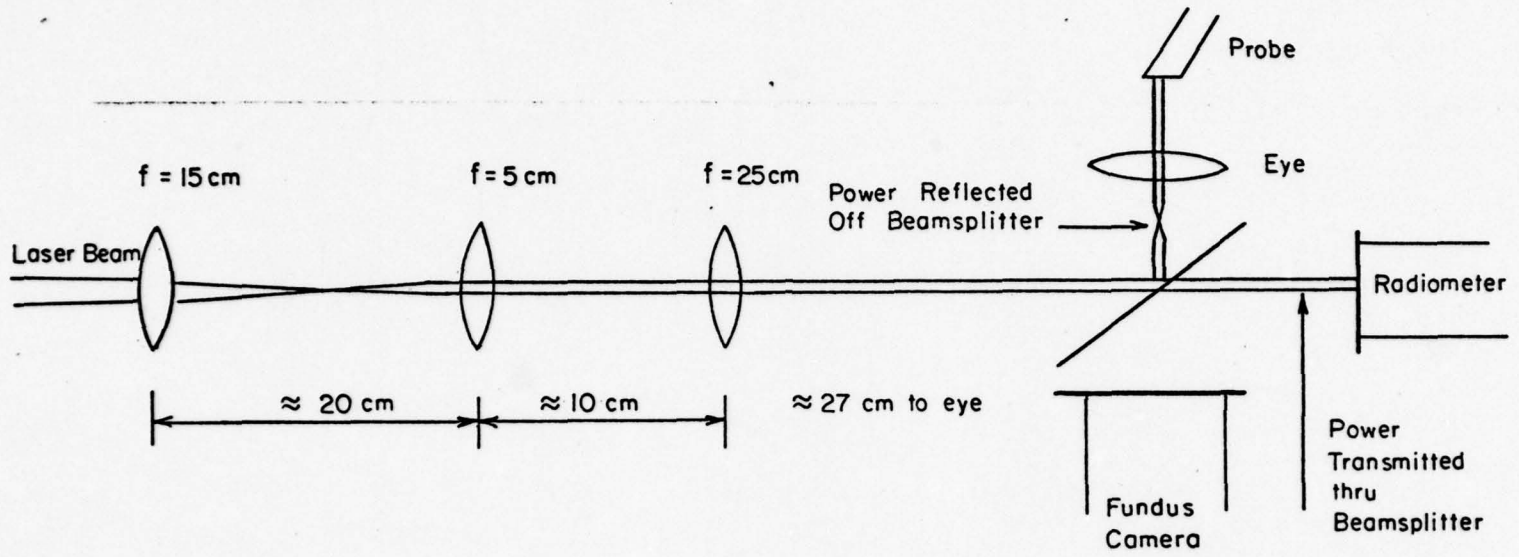

Figure 3. Optical Configuration for Measuring the Transmission of the Ocular Media with a 600 Micron Diameter Fiber Optic Probe.

voltage of the probe-detector was therefore determined for a given laser power incident on the probe tip.

The reflection of light at the contact lens - air interface and at the contact lens - cornea interface was calculated by Kidwell (7) to be very nearly 3%. The measurement of the power incident on the contact lens therefore was reduced by 3% prior to calculation of the ratio of power inside the eye to power incident on the eye. The formula for calculating the transmission of the ocular media is therefore:

$$T.O.M. = \frac{(\text{Probe Output, mV})(\text{Probe Calibration, W/mV})}{(\text{Incident Corneal Power, W})(0.97)} \quad (1)$$

Minimal Image -- Transfer Function

Illumination -- Point Source

The minimal image or point spread function, from which the transfer function for the eye may be derived, can be obtained by illuminating the cornea with a uniform plane wave.

The "uniform plane wave" requires a near constant light amplitude across the cornea as well as a nearly flat phase curvature. A TEM laser beam has a gaussian amplitude profile, and a phase curvature related to the beam divergence. If the beam is expanded and recollimated, both the amplitude and phase requirements can be satisfied.

The collimated beam approximates a uniform plane wave according to the diffraction theory relationships developed in Seigman (10).

Six laser wavelengths were used in the minimal image measurements. The argon laser provided 455.5 nm, 488 nm, and 514.5 nm; the dye laser, pumped by the argon, with Rhodamine 6G dye, provided wavelengths of approximately 560 nm, 590 nm, and 630 nm.

The dye laser is configured such that wavelength selection is quickly and easily accomplished by means of a movable tuning wedge within its optical cavity. Wavelengths from the argon laser were selected by means of narrowband interference filters. Minimal time was required to change wavelengths during an experiment.

Illumination -- Line Source

The light source used to form a line image on the retina was the same as that used by Robson and Enroth-Cugell (9), a Chicago Miniature CM8-52. This lamp had a ribbon filament which measured 81 mm by 0.51 mm. It was mounted vertically 4 meters from the eye. The width of the filament thus subtended 25.7 arc seconds at the eye.

The lamp filament was operated at a current of 4.8A (18.9V) to give a color temperature of 2900 degrees C. The spectrum of the output light under this condition, as determined by Robson and Enroth-Cugell, was centered at approximately 600 nm with a bandwidth of 220 nm, neglecting the infrared output.

Eye Preparation

The animal was prepared surgically as described previously. Special care was taken in handling the eye for these experiments so that minimal damage or trauma occurred. The eye was examined frequently through the fundus camera during the experiment to determine the condition of the optics and the fundus.

Since the eyelid was held open during the experiment which lasted several hours, a hard contact lens was used to keep the cornea from drying. The curvature of the lens was based on measurements of a sample of monkey eyes. A set of lenses was obtained having the measured curvature in powers of +1, -1, +1.5, -1.5, +2, +2.5, +3, and +3.5 Diopters (D). The lenses were used in focusing the image in the eye at the probe tip. Barnes-Hine contact lens wetting solutions and artificial tears were used with the lenses. Deionized water was used to rinse the front surface of the lens after placement in the eye.

The pupil was dilated and accomodation paralyzed with Neo-Synephrine during the surgical preparation. Some of the minimal images were scanned with no artificial pupil; others were scanned with an artificial pupil of 4,3, 2, or 1 mm diameter placed directly in front of the eye, centered on the cornea.

Probe

The fiber optic probes used in these experiments were typically 10 to 15 microns in tip diameter. They were silvered and copper coated as described in the probe development section. The sensitivity of the photomultiplier tube proved to be very

convenient since only a small portion of the collimated laser beam entered the eye and excessive laser power was not required even though the light levels in the eye were relatively low. The photomultiplier was especially valuable in measuring the images of the line source. The spectral response of the photomultiplier was sufficient for all of the visible wavelengths employed, and effectively filtered any near infrared or longer wavelength light.

The depth of the probe was not determined exactly, but the tip of the probe was visible well in front of the neural layers. Table 1 shows the displacement of the focal plane with respect to focus error (or dioptric correction) in a monkey with typical total refractive power of 72.6D. The position of the probe tip with respect to the eye's natural focal plane would have an effect on the corrective lens required for optimum focus.

Scans -- Point Image

The image was usually placed on the micro probe tip while viewing the fundus and also watching the oscilloscope for the signal to appear. Once the image was located, the central peak was found by adjusting the stereotaxic apparatus in both the horizontal and vertical directions. The image was then rotated off the probe, the stepping motor was reversed, and a scan was made, moving one horizontal motor step (25 arc seconds) between each shutter pulse of approximately .25 second duration. The intensity profiles were filtered and recorded on a Brush chart recorder.

TABLE 1

Focal Plane Displacement with respect to

Focusing Error in the Rhesus Monkey Eye

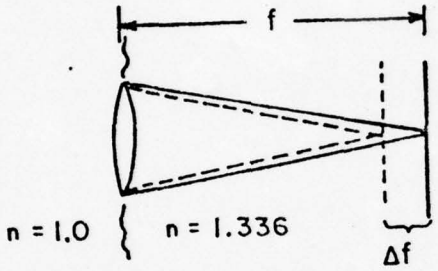

Uncorrected Power = 72.6 D

f = 18.4 mm

Focus Error, D	Total Power, D	f, mm	Δf, mm
0	72.6	18.40	0
+1.5	74.1	18.03	0.370
+2.0	74.6	17.91	0.490
+2.5	75.1	17.79	0.610
+3.0	75.6	17.67	0.730
+3.5	76.1	17.56	0.840

Scans -- Line Images

The line images were scanned in similar fashion as the point images. A vertical peak was located, although it was broader than the vertical peak of the point images. The scan was taken one motor step at a time. The width of the image was determined from the chart record; steps were taken once per second and the chart moved one millimeter per second.

For both the point images and the line images, the first scan was made with a 0 diopter contact lens and no artificial pupil on the eye. Contact lenses of increasing power were placed on the eye for subsequent scans. The lens which produced the narrowest image (as measured between the half-height points) was considered to be optimum. The "optimum focus" was obtained with the optimum lens and a slight tweaking of the hydraulic microdrive which varied probe depth in 2 micron increments.

When the "optimum focus" was found, scans were made with 4, 3, 2, and 1 mm pupils placed directly in front of the eye and centered on the cornea. In the case of the laser -- point images, scans were made at six wavelengths.

Data Analysis -- Line Images

The data were corrected for the effect of using a finite-size probe in sampling the image. The measured image was considered a convolution of the probe (a circular aperture) with a "true" image. The Fourier transform of the measured image was therefore a product of the transforms of the circular aperture and the "true" image.

The "true" image was obtained by dividing the transform of the measured image by the transform of a circular aperture. The transform of the aperture was smoothed to avoid dividing by zero.

The method was tested using a gaussian fuction, σ = 1 arc minute, as a hypothetical "true" image profile. This function was perturbed by multiplying its transform by the transform of the circular aperture and taking the inverse transform. The original and perturbed profiles are shown in Figures 4 and 5, where it can be noted that the width between half height points is approximately 10% larger than the original profile.

The transform of the corrected profile is the product of: the transform of the original function, the transform of the circular aperture, the truncated inverse function, and the smoothing function. The corrected profile, found by taking the inverse Fourier transform of the above, is shown in Figure 6. The width between half height points is within 2% of the original function.

The transforms of corrected line image profiles were obtained from the products of: the transform of the measured image ("raw" data points from the chart records with sufficient zeroes supplied to make 128 points per profile were transformed using a one dimensional FFT routine), the truncated inverse function, and the smoothing function. The corrected line image profiles were obtained by inverse Fourier transformation. Each of the 128 points in the arrays corresponded to one motor step, or 25 arc seconds. The laser beam was displaced approximately 2.3 microns at the

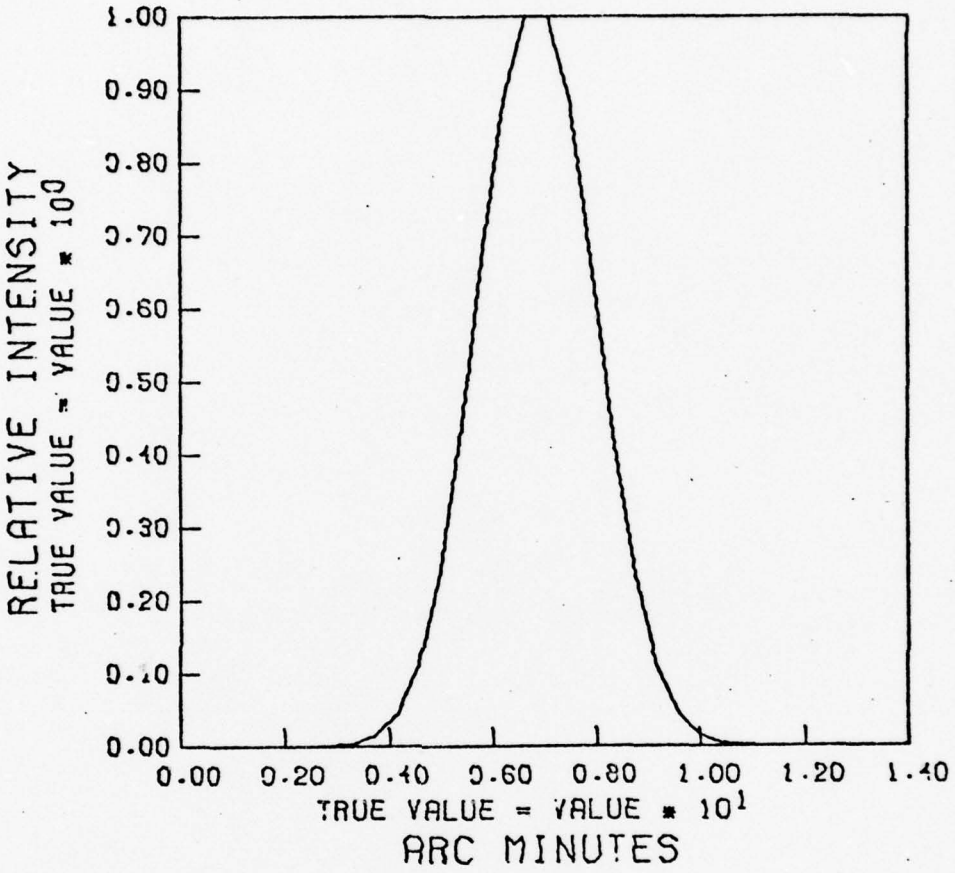

ORIGINAL FUNCTION

Figure 4. Original Gaussian Function.

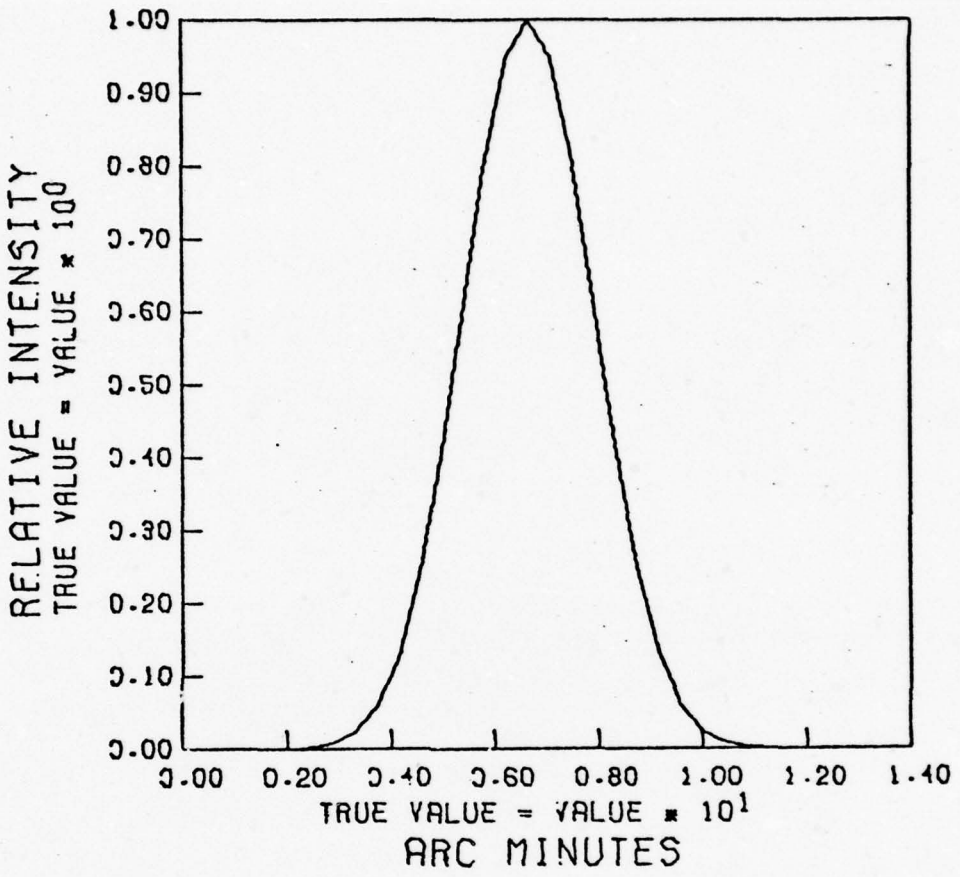

PERTURBED FUNCTION

Figure 5. Gaussian Function Perturbed by Sampling with a Circular Aperture.

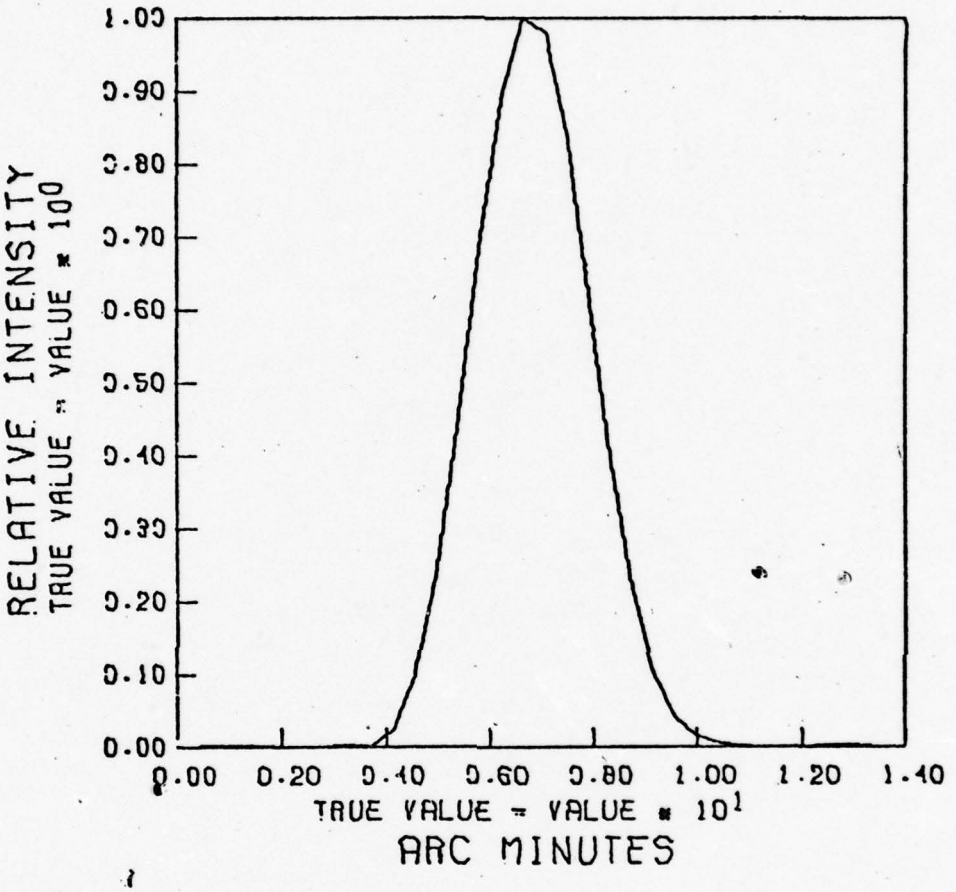

Figure 6. Perturbed Gaussian Function Restored by Inverse Filtering Technique.

retina per step. The 14 micron aperture used in the scans therefore corresponded to 6 points in the 128 point array.

The width of the line filament (.51 mm at 4 M) was approximately 25 arc seconds, or one point of the 128 point array. This width had a negligible effect on the measured profile compared to the effect of the probe.

Data Analysis -- Point Images

The analysis discussed for the line images can be extended to two dimensions. In this case, since only a one-dimensional cross section of the point images was obtained, an estimate of the amount of spread in the measured image was calculated by using a two dimensional gaussian profile. This estimate would then suggest that the measured images were larger than the "true" images by some approximate amount. If the measured images were "corrected" as in the case of the line images, the entire two dimensional image profile would be needed.

The spread of image profiles depends on the ratio of the image profile diameter to the probe diameter. Table 2 shows the per cent spread of gaussian image profiles for probe diameters of 1σ, 2σ, 5σ, and 10σ with respect to the beam standard deviations, σ. If the measured image was corrected for probe perturbations the 12% increase in half height associated with 2σ probe diameter would be reduced to one percent.

TABLE 2.

Spread of Two Dimensional Gaussian Profiles due to Finite Probe Size

Probe Diameter	Per Cent Increase in Half-Height Width
1σ	5%
2σ	12%
5σ	50%
10σ	125%

RESULTS

Line Images

Images of the tungsten line filament described previously were obtained in three monkey eyes, numbered 9877, 02077 and 121677.

The first task once the filament image was placed on the probe tip in the monkey eye was to scan the image with contact lenses of varying powers so as to find the best focus. Figure 7 shows four scans at lens powers of 0 D, +1.5 D, +2 D, and a repeat at +1.5 D for Monkey 9877. The scan at +1.5 D was narrowest between half height points, and was therefore considered the "best" focus.

Figure 8 shows scans at +1.5 D, +2 D, +2.5 D, +3 D, and +3.5 D for Monkey 92077. Another scan is shown at +3.5 D after the probe had been driven inward slightly (10 to 20 microns), producing a still smaller image. This image was accepted as the "best" focus, since no higher power corrective lenses were available.

The retina of Monkey 121677 had detached prior to probe insertion; often it was difficult to insert a probe past the detached tissue layers. In this monkey, instead of the small hole in the sclera, a large hole was cut with a scalpel so the probe could be completely inserted into the eye. Only a small amount of vitreous humor leaked out of the eye; it remained

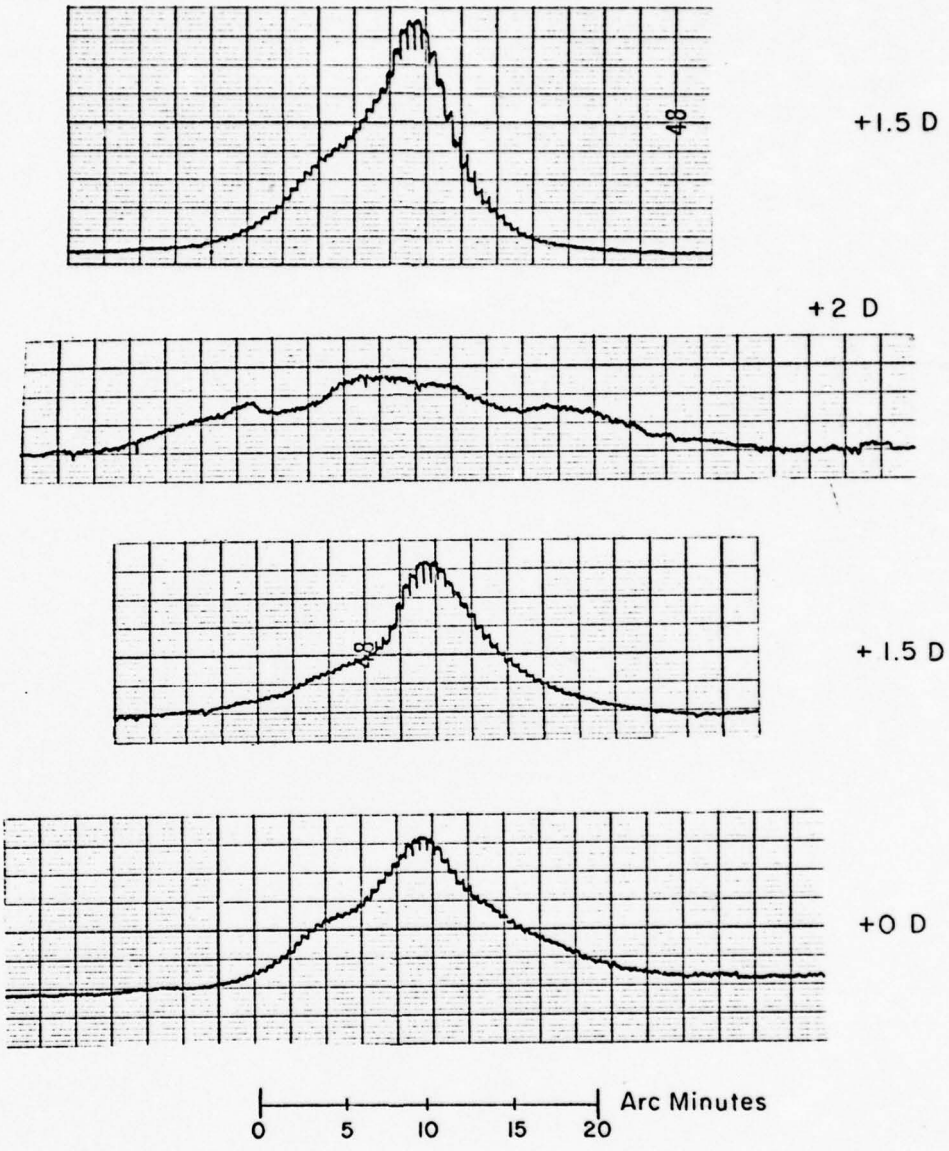

Figure 7. Monkey 9877 Misfocused Scans at Corrective Lens Powers Shown.

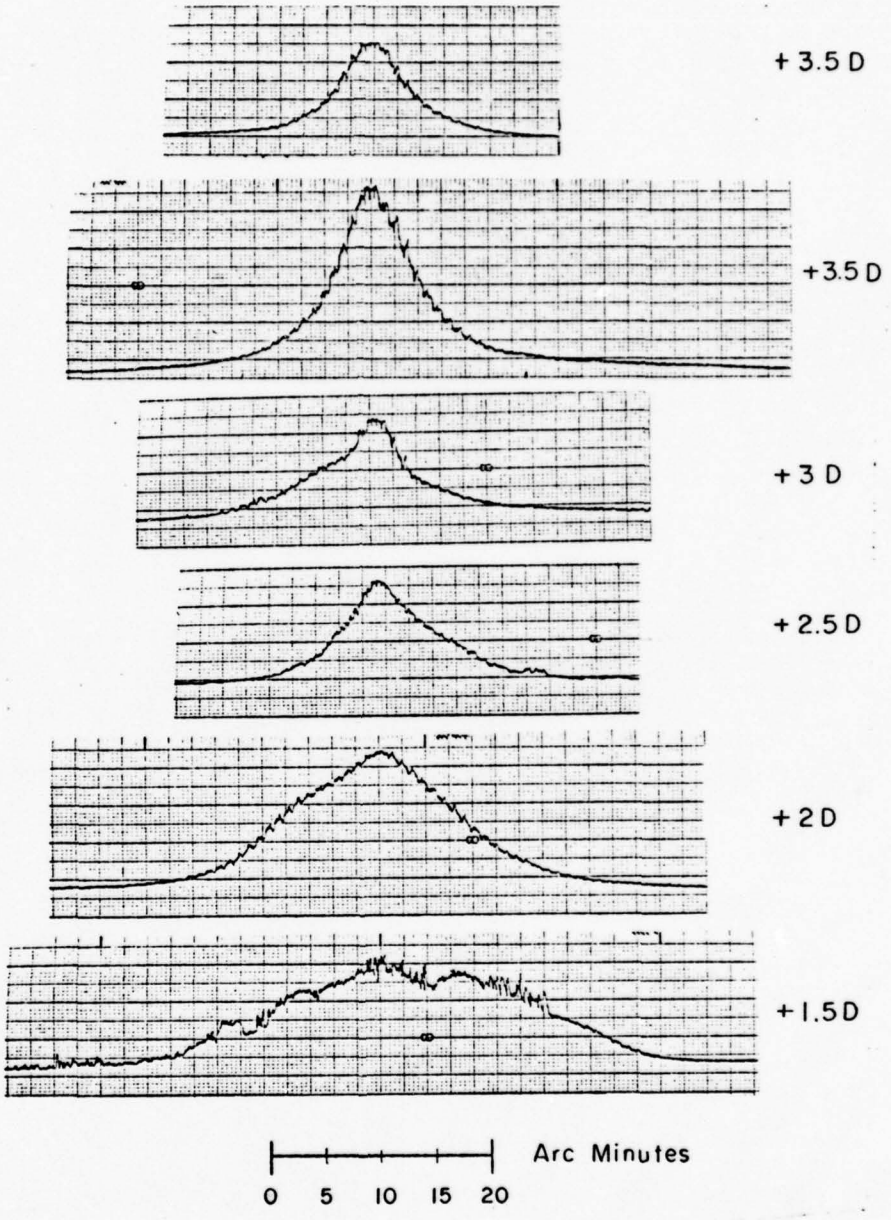

Figure 8. Monkey 92077 Misfocused Scans at Corrective Lens Powers Shown.

otherwise intact. The "optimum focus" was found with a +2.5 D lens by moving the probe in and out with the micromanipulator.

For each monkey, scans were taken at "best" focus with no artificial pupil, and also for pupils of 4, 3, 2, and 1 mm centered directly in front of the cornea. The data were digitized directly from the chart records for input to the computer. The images were corrected for the finite probe size by the method described earlier, and are shown in Figures 9 through 11. These corrected images are estimates of the eye's line spread function for each pupil condition.

The normalized Fourier transforms of the corrected image profiles are shown in Figures 12 through 14. These transforms represent estimates of the eye's modulation transfer function for each pupil condition.

A criterion relating optical resolution of the eye to the line spread function is the relative width of the line spread function profile. The widths between half height points of the corrected image profiles, in arc minutes, for the three monkeys and all pupil conditions are given in Table 3.

Point Images

Retinal images formed by expanded, collimated laser beams (see previous description in Experimental Procedure section) were obtained from two monkeys, numbered 72177 and 10477.

The "best" focus was found in the same way as for the line images. In Figure 15, scans are shown at corrective lens powers

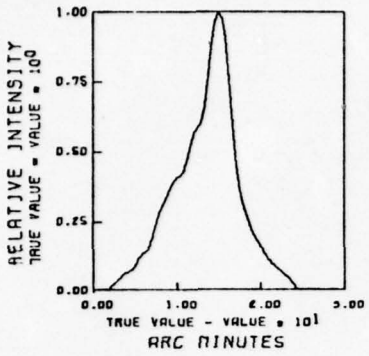

No Pupil

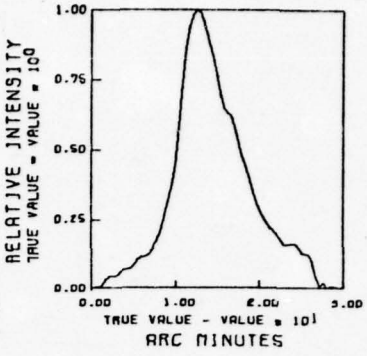

4 mm Pupil

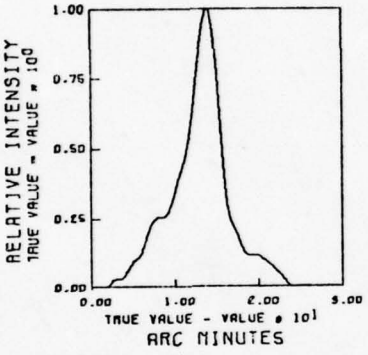

3 mm Pupil

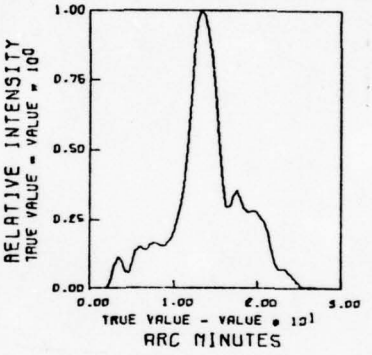

2 mm Pupil

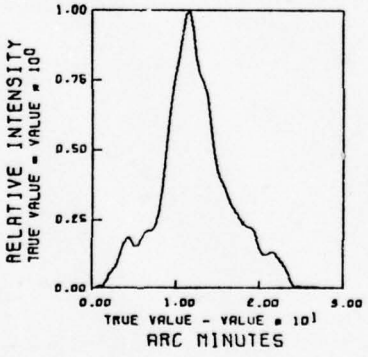

1 mm Pupil

Figure 9. Monkey 9877 Corrected Line Images at Artificial Pupil Sizes Shown.

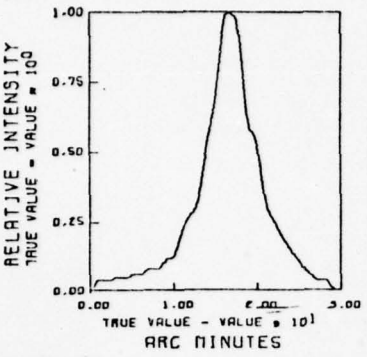

No Pupil

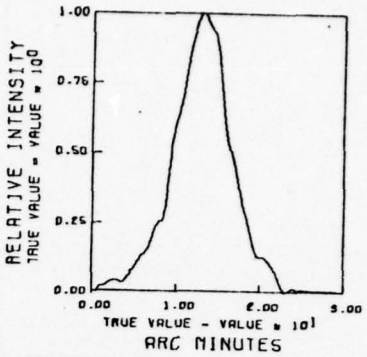

4 mm Pupil

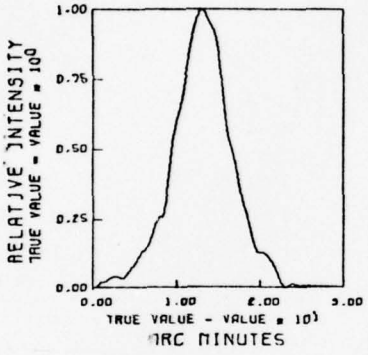

3 mm Pupil

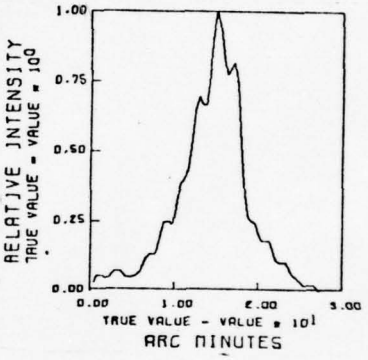

2 mm Pupil

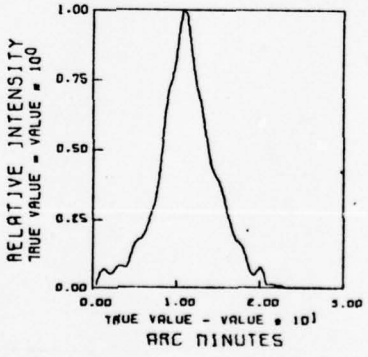

1 mm pupil

Figure 10. Monkey 92077 Corrected Line Images at Artificial Pupil Sizes Shown.

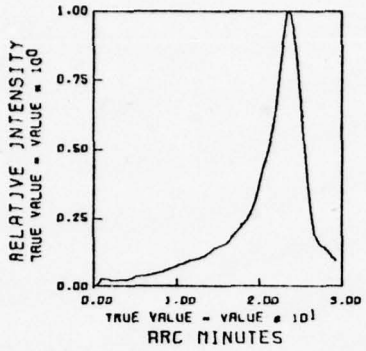

No Pupil

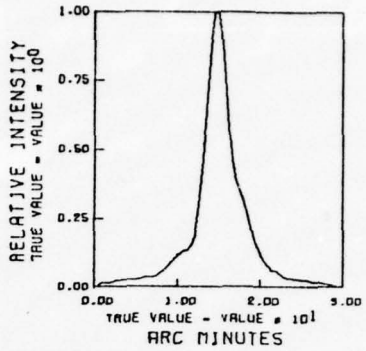

4 mm Pupil

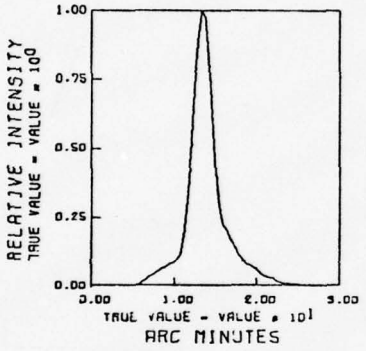

3 mm Pupil

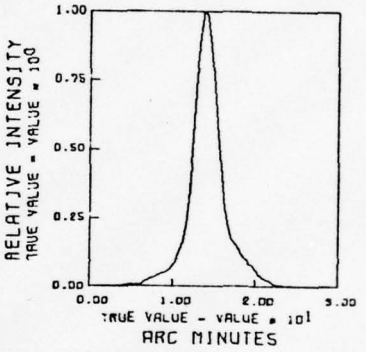

2 mm Pupil

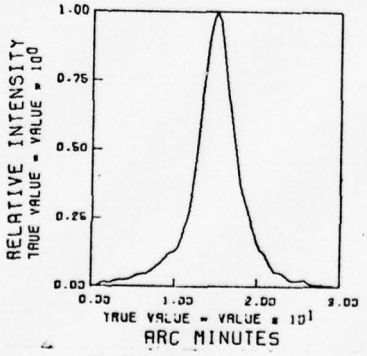

1 mm Pupil

Figure 11. Monkey 121677 Corrected Line Images at Artificial Pupil Sizes Shown.

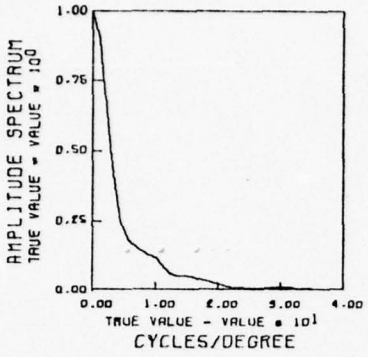

No Pupil

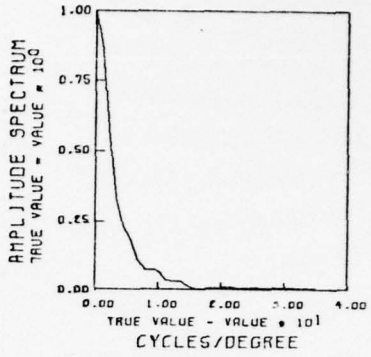

4 mm Pupil

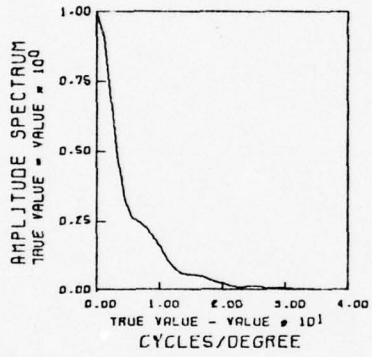

3 mm Pupil

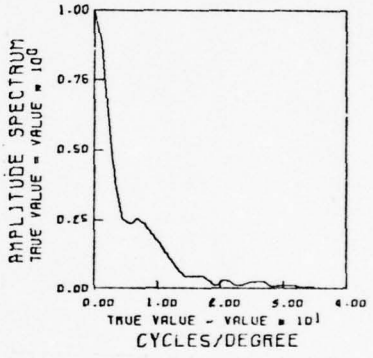

2 mm Pupil

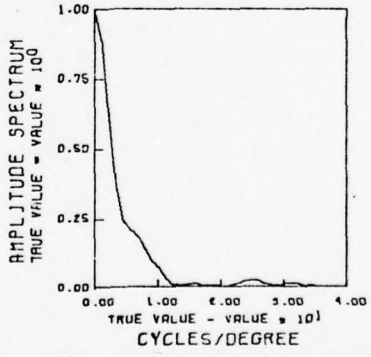

1 mm Pupil

Figure 12. Monkey 9877 Amplitude Spectra from Corrected Line Images at Artificial Pupil Sizes Shown.

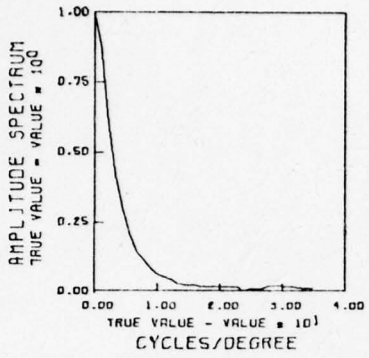

No Pupil

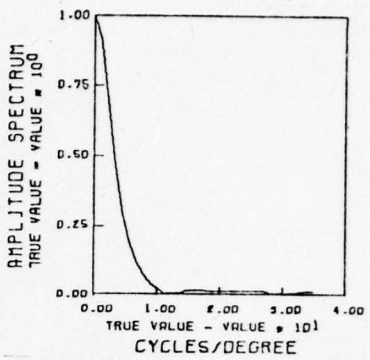

4 mm Pupil

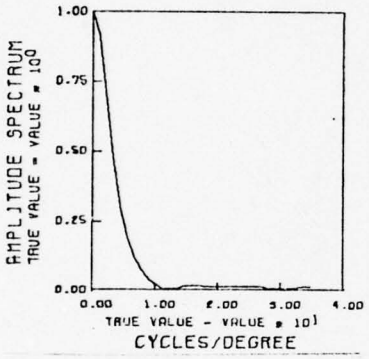

3 mm Pupil

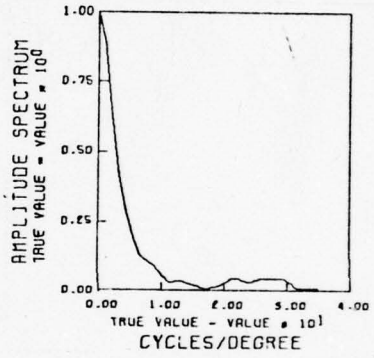

2 mm Pupil

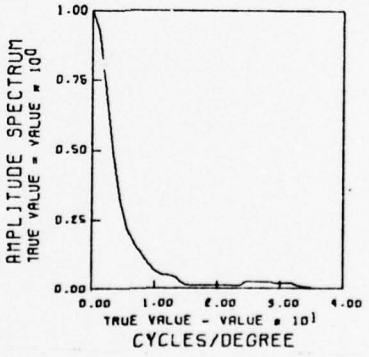

1 mm Pupil

Figure 13. Monkey 92077 Amplitude Spectra from Corrected Line Images at Artificial Pupil Sizes Shown.

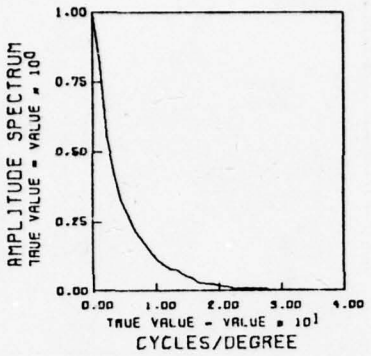

No Pupil

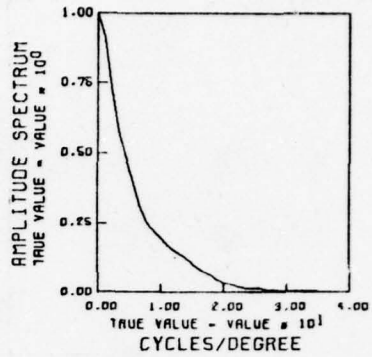

4 mm Pupil

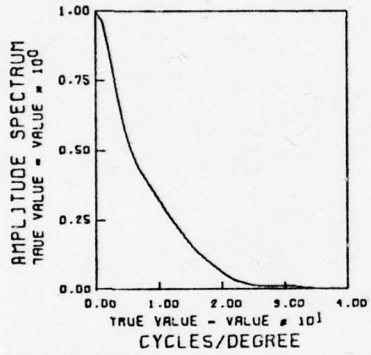

3 mm Pupil

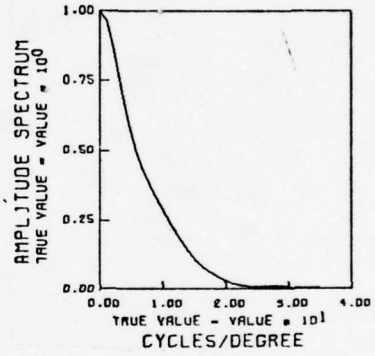

2 mm Pupil

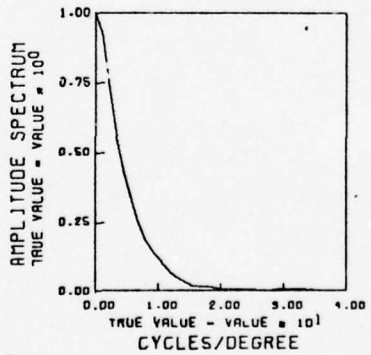

1 mm Pupil

Figure 14. Monkey 121677 Amplitude Spectra from Corrected Line Images at Artificial Pupil Sizes Shown.

TABLE 3

Widths between Half-Height Points

for Corrected Line Images

Monkey	Pupil Condition	Width between Half-Height Points (Arc Minutes)
9877	No Pupil	5.5
	4 mm	7.6
	3 mm	4.1
	2 mm	3.9
	1 mm	5.8
92077	No Pupil	6.2
	4 mm	7.2
	3 mm	7.2
	2 mm	6.1
	1 mm	5.6
121677	No Pupil	4.4
	4 mm	3.2
	3 mm	2.8
	2 mm	3.1
	1 mm	4.8

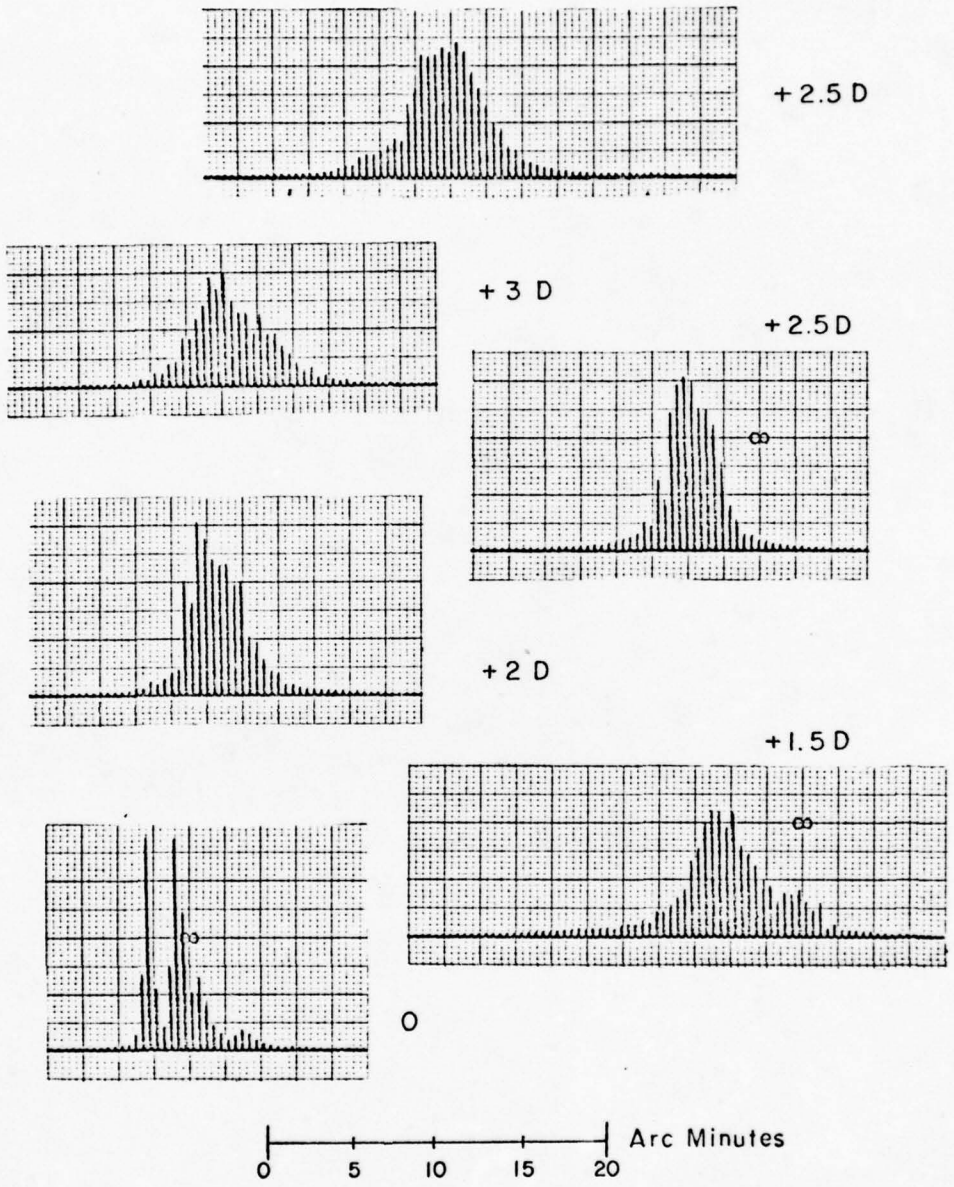

Figure 15. Monkey 10477 Misfocused Point Images at Corrective Lens Power Shown.

of 0 D, +1.5 D, +2 D, +2.5 D, +3 D, and a repeat at +2.5 D for monkey 10477. The +2.5 D correction was considered "best", even though the repeated scan gave a larger image than the first scan. The image was still smaller than the +3 D image. The wavelength employed for these scans was 514.4 nm.

For monkey 72177, the "best" focus was found at approximately 590 nm, and scans were then taken at approximately 630 nm, and at approximately 560 nm, with no artificial pupil. Since the probe was at the same depth, these scans attempted to measure a change in the point image with respect to wavelength; i.e., to attempt to demonstrate a chromatic aberration effect in the eye.

Returning to the red wavelength (630 nm), the probe was driven in and out slightly and scans were taken until an image slightly smaller than the previous one was obtained. Scans were then made with 4, 3, 2, and 1 mm artificial pupils. With the 1 mm pupil in place, the wavelength was changed to blue (488 nm), purple (455.5 nm), and green (514.4 nm). The scans for monkey 72177 are shown in Figures 16 and 17.

For monkey 10477, when the "best" focus was found, scans were taken at 514.5 nm, 488 nm, and 455.5 nm with no artificial pupil, and pupils of 4, 3, 2, and 1 mm centered in front of the cornea. The scans for monkey 10477 are shown in Figures 18 through 20.

The preceding scans were digitized directly from the chart records for computer plotting.

The widths between half height points, shown in Table 4, are slightly larger in the measured image profiles than they

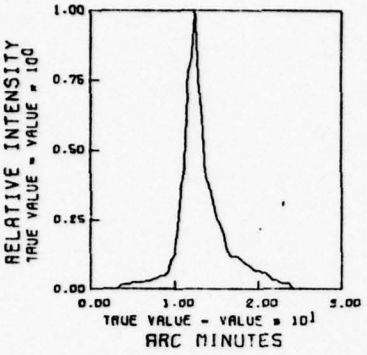

No Pupil

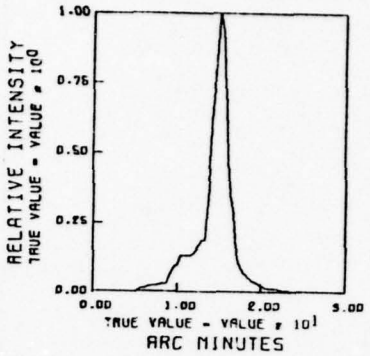

4 mm Pupil

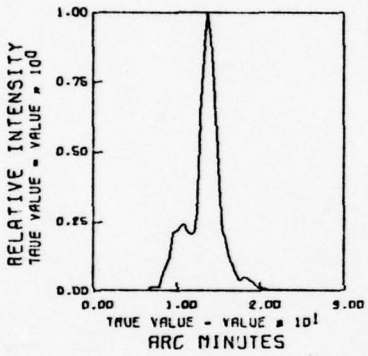

3 mm Pupil

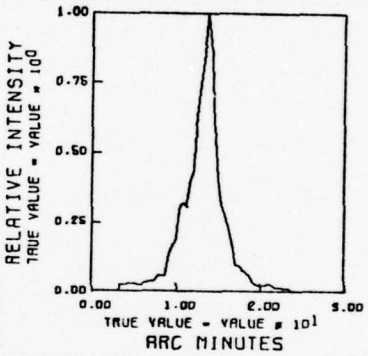

2 mm Pupil

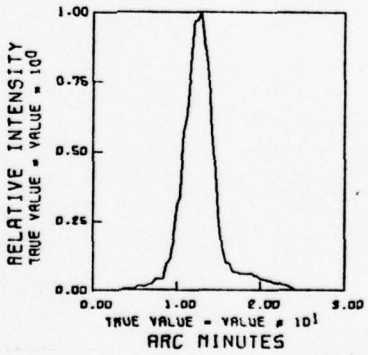

1 mm Pupil

Figure 16. Monkey 72177 Point Images at 630 nm at Artificial Pupil Sizes Shown.

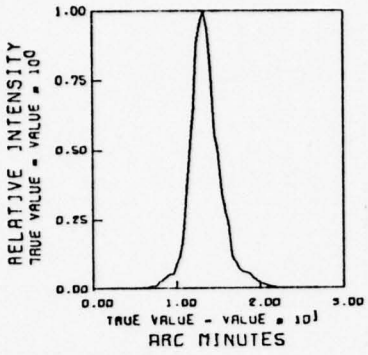

No Pupil 590 nm

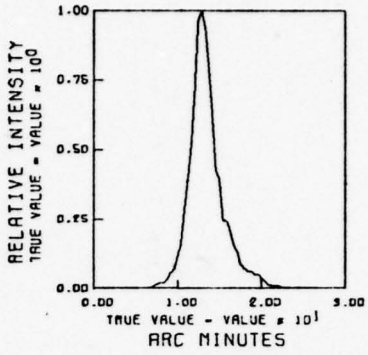

No Pupil 560 nm

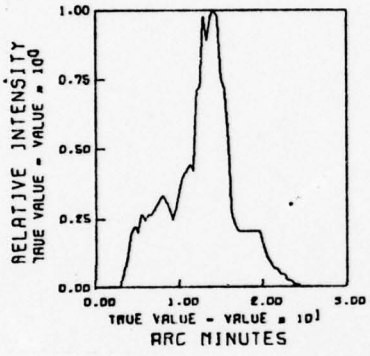

1 mm Pupil 514.5 nm

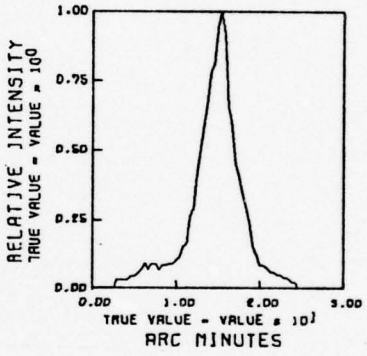

1 mm Pupil 488 nm

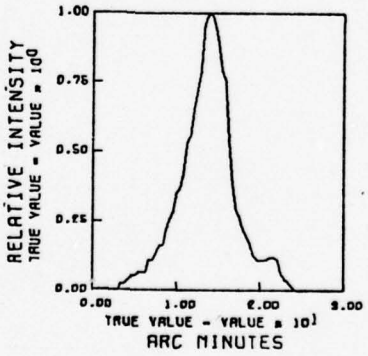

1 mm Pupil 455 nm

Figure 17. Monkey 72177 Point Images at Wavelength and Artificial Pupil Sizes Shown.

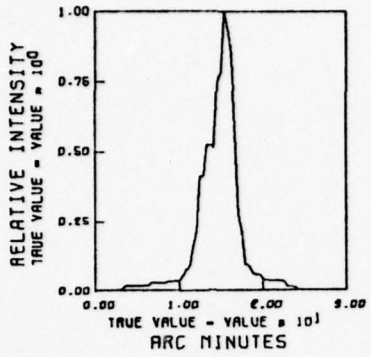

No Pupil

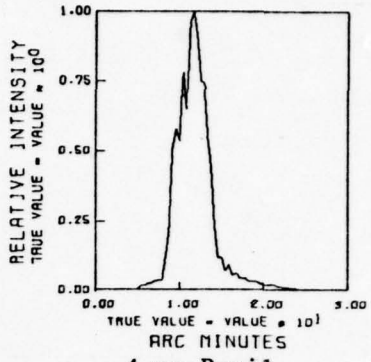

4 mm Pupil

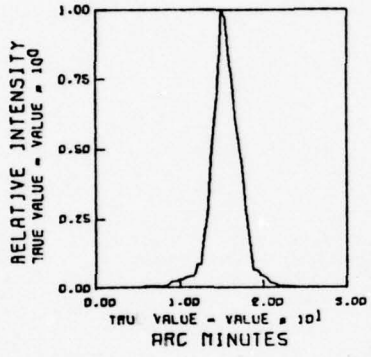

3 mm Pupil

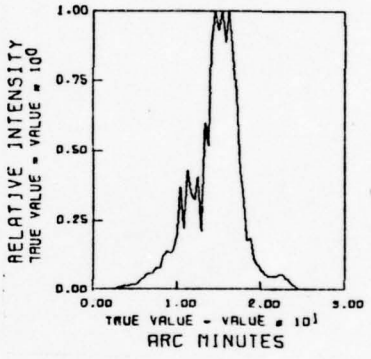

2 mm Pupil

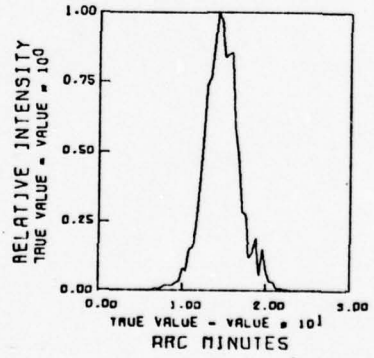

1 mm Pupil

Figure 18. Monkey 10477 Point Images at 455.5 nm at Artificial Pupil Sizes Shown.

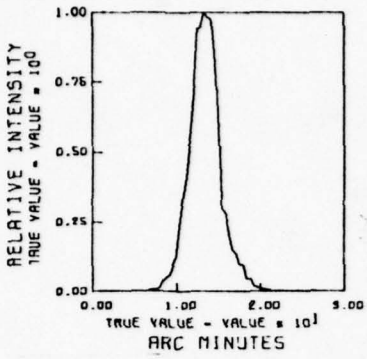

No Pupil

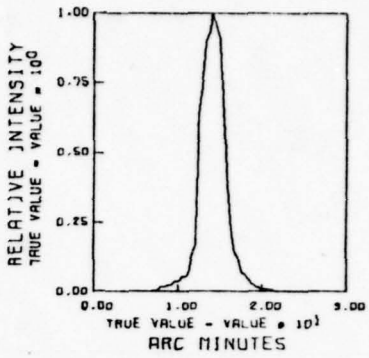

4 mm Pupil

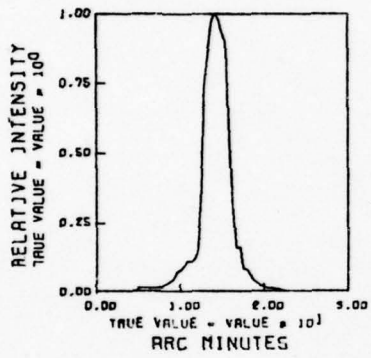

3 mm Pupil

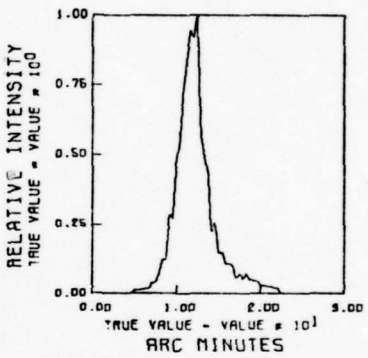

2 mm Pupil

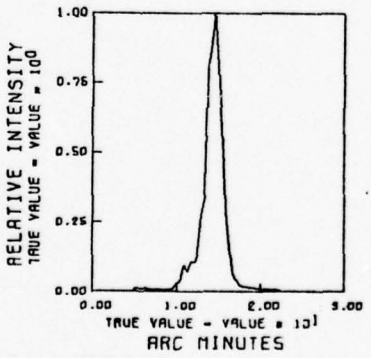

1 mm Pupil

Figure 19. Monkey 10477 Point Images at 488 nm at Artificial Pupil Sizes Shown.

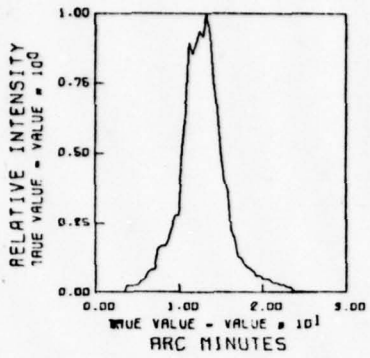

No Pupil

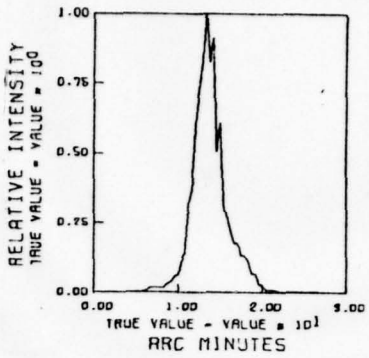

4 mm Pupil

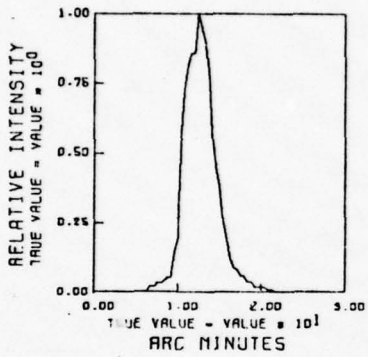

3 mm Pupil

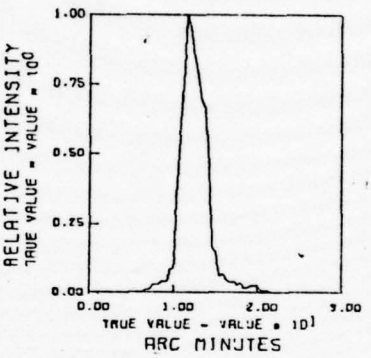

2 mm Pupil

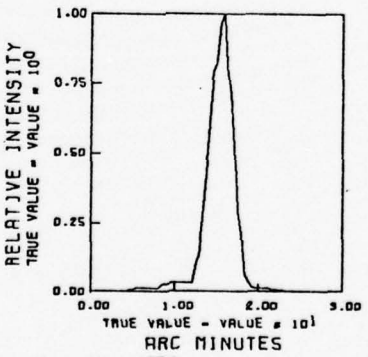

1 mm Pupil

Figure 20. Monkey 10477 Point Images at 514.5 nm at Artificial Pupil Sizes Shown.

TABLE 4

Widths between Half-Height Points for Point Images

Monkey	Pupil	NM	Width between Half-Height Points (arc min)	Probe Corr. Factor	Corrected Width Arc Min
72177	None	630	2.2	0.9	1.98
	4 mm	630	2.0	0.9	1.8
	3 mm	630	2.2	0.9	1.98
	2 mm	630	2.5	0.9	2.25
	1 mm	630	3.8	0.92	3.5
	None	590	3.2	0.9	2.88
	None	560	2.8	0.9	2.52
	1 mm	514.5	4.2	0.93	3.91
	1 mm	488	4.0	0.93	3.72
	1 mm	455.5	5.3	0.95	5.04
10477	None	514.5	4.8	0.94	4.51
	4 mm	514.5	3.1	0.9	2.79
	3 mm	514.5	4.0	0.93	3.72
	2 mm	514.5	3.3	0.9	2.97
	1 mm	514.5	3.0	0.9	2.7
	None	488	3.6	0.91	3.28
	4 mm	488	3.2	0.9	2.88
	3 mm	488	3.2	0.9	2.88
	2 mm	488	3.0	0.9	2.7
	1 mm	488	2.0	0.9	1.8
	None	455.5	3.4	0.9	3.06

4 mm	455.5	4.4	0.93	4.09
3 mm	455.5	3.1	0.9	2.79
2 mm	455.5	4.2	0.93	3.91
1 mm	455.5	4.2	0.93	3.91

would be in the "true" image profiles due to the finite size of the probe. The analysis of the two dimensional gaussian profiles discussed in the Experimental Procedure section shows that the probe spreads the image by an amount up to 10% for the smallest images encountered here. The widths of the measured image profiles, reduced by the appropriate scaling factors determined from the analysis, are also shown in Table 4.

For the modulation transfer function to be obtained directly from a point image profile, the complete two dimensional profile of the point image is required. If the two dimensional profile is known, or if the one dimensional profile can be considered to be circularly symmetric, the modulation transfer function can be obtained by performing a Fourier transformation in two dimensions. Alternatively, a line spread function can be calculated from a superposition of point spread functions (6), and a one dimensional Fourier transformation can be performed on that function.

Transmission of the Ocular Media

Measurements of the transmission of the ocular media were made in two rabbits and two rhesus monkeys at wavelengths of 455.5 nm, 488 nm, 514.5 nm, 560 nm, 590 nm, 630 nm, and 1060 nm. The measurements were made with the 600 micron aperture probe.

The rabbit data are shown along with the rabbit ocular transmission curve of Geeraets and Berry (3) in Figure 21. The data from one monkey (32178) are shown in Figure 22, along with the

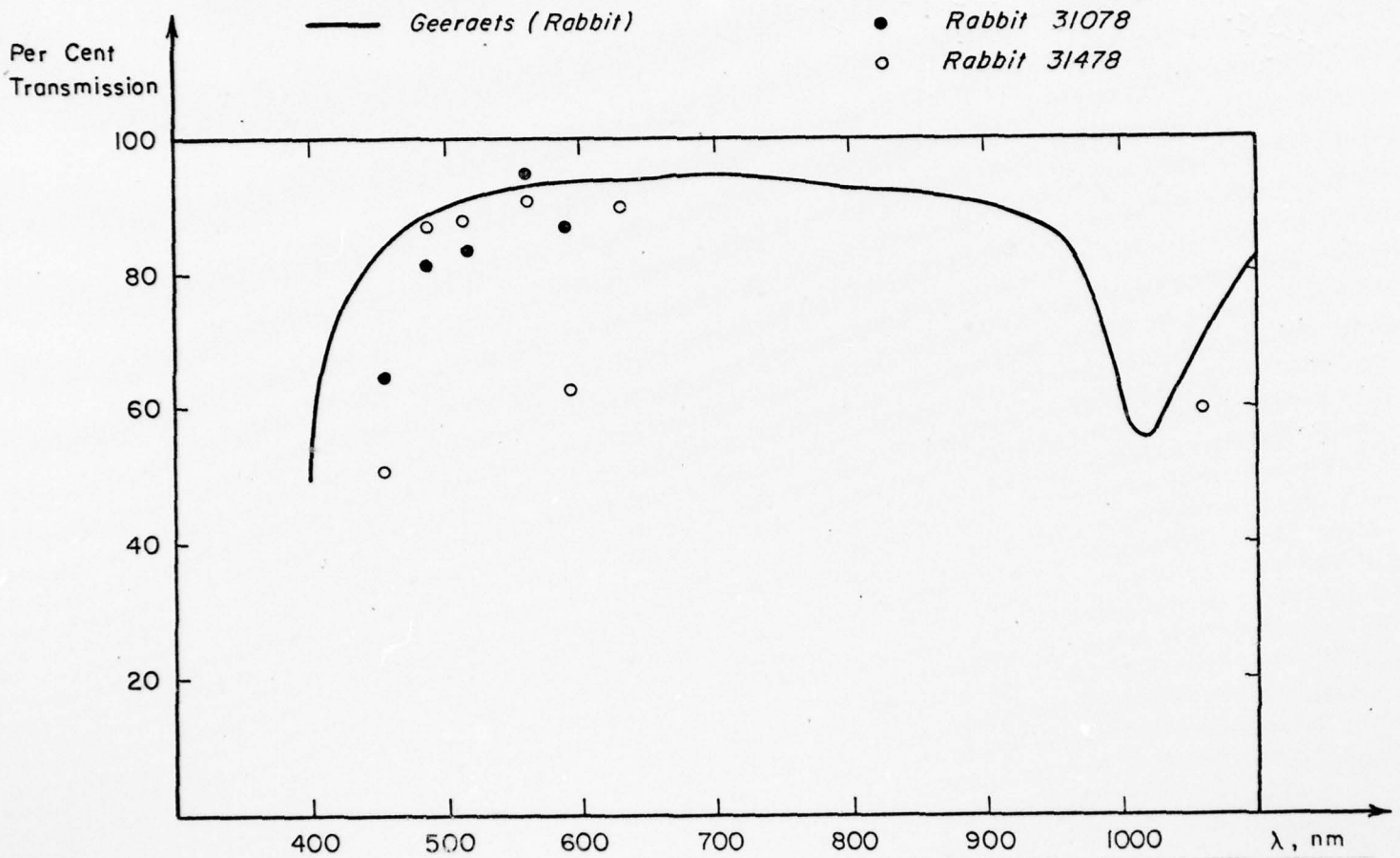

Figure 21. Transmission of the Ocular Media from Two Rabbits Plotted with Curve of Geeraets and Berry.

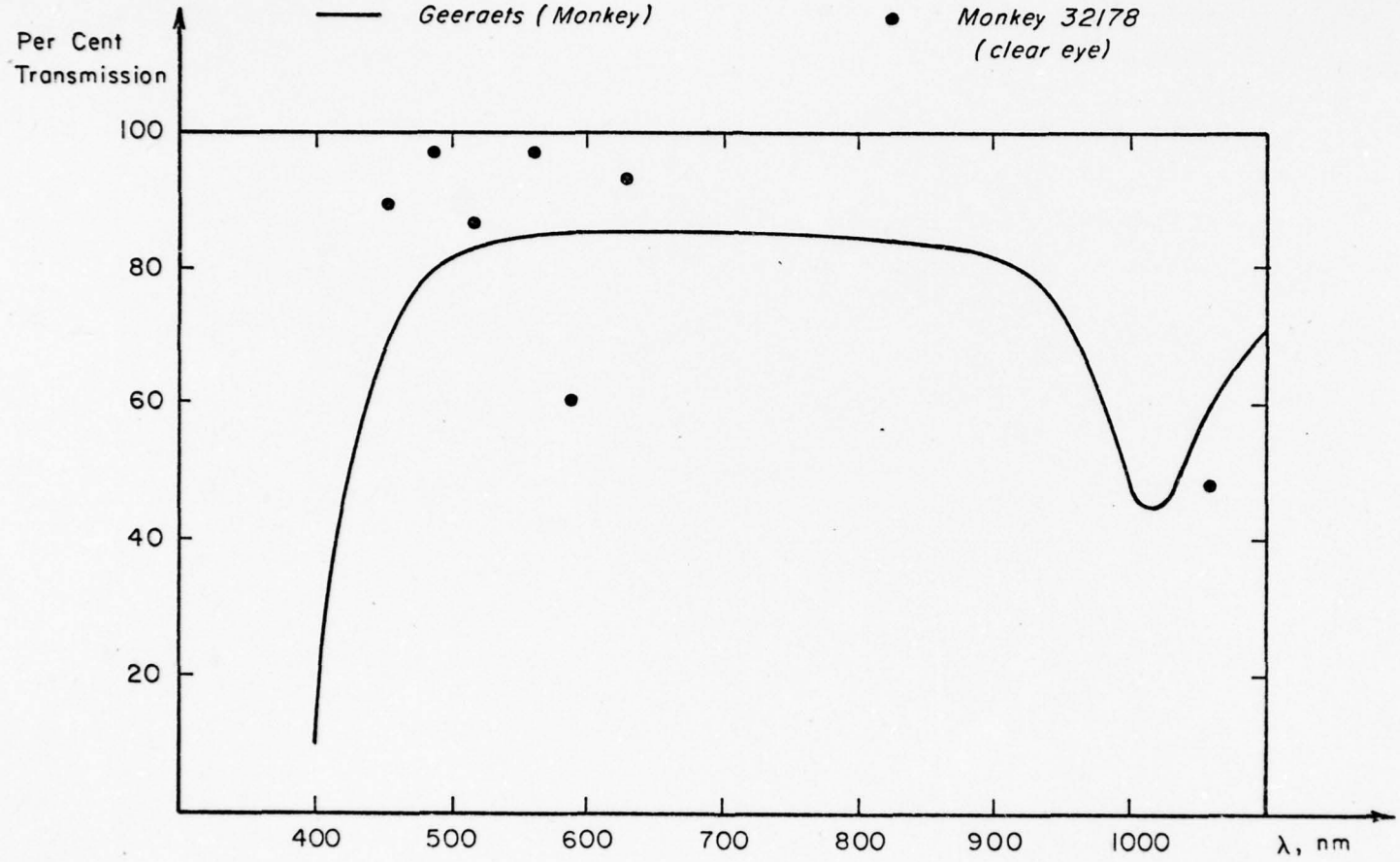

Figure 22. Transmission of the Ocular Media from One Monkey Plotted with Curve of Geeraets and Berry.

monkey ocular transmission curve of Geeraets and Berry. The cornea of the second monkey (31778) clouded early in the experiment and remained so throughout; the reduced transmission values are shown in Figure 23 with the curve of Geeraets and Berry.

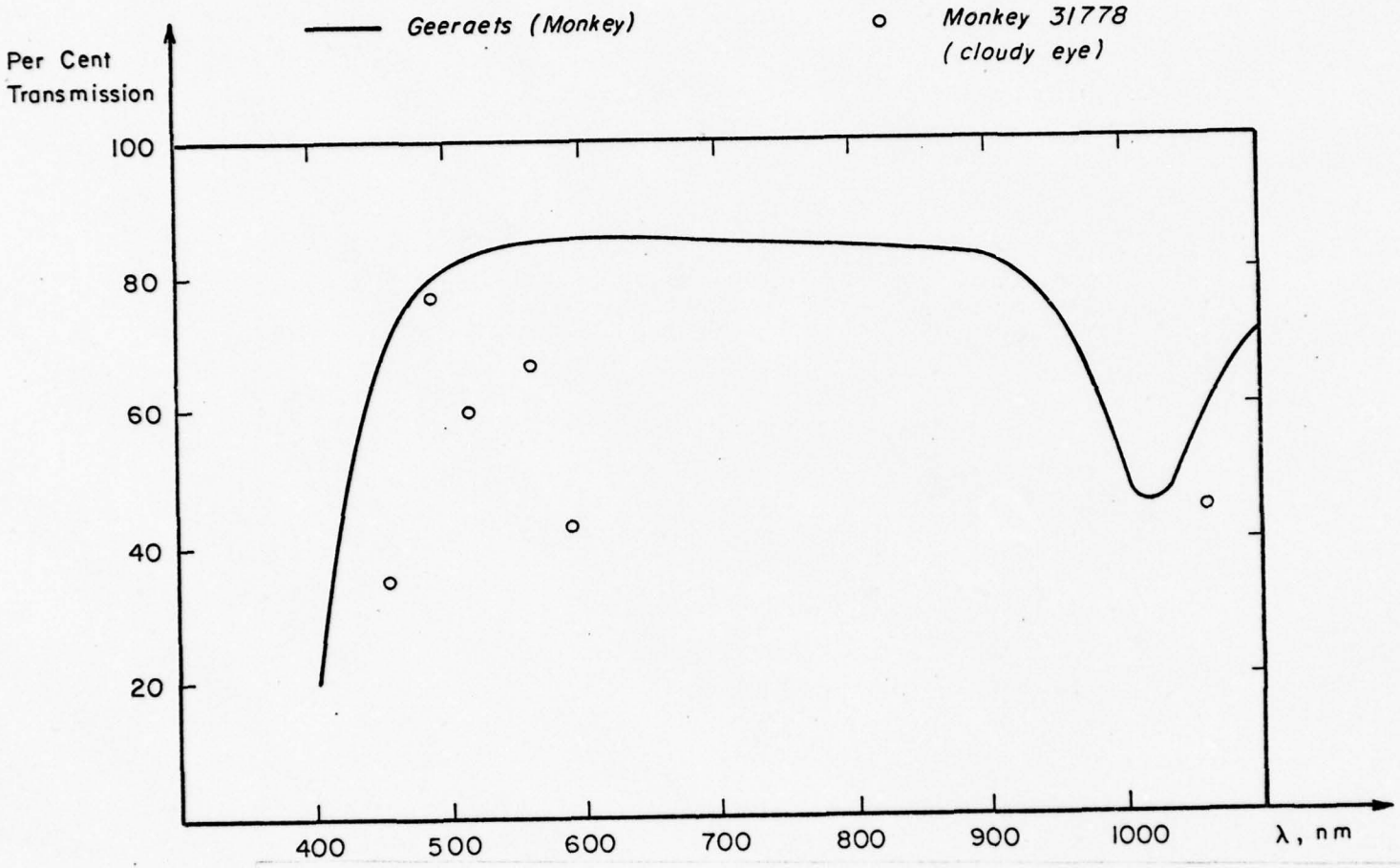

Figure 23. Transmission of the Ocular Media from One Monkey Whose Cornea Had Clouded Plotted with Curve of Geeraets and Berry.

DISCUSSION

Line and Point Images

There is no clear cut relationship of the widths between half-height points of the measured line images and the sizes of the artificial pupils. One point (Monkey 9877, 2 mm pupil) is very close to the data of Enroth-Cugell for the same pupil condition in the cat. The images for no pupil are slightly better than those of Enroth-Cugell. For Monkey 92077, the image profiles may not represent the "best" focus for the eye, since they are typically 50 to 60% larger than the images of Monkey 9477, and the attempts at finding the best focused image ended with the use of a +3.5 Dipter contact lens, the strongest on hand. The data from Monkey 121677 are better than all those of Enroth-Cugell for the cat except for the 1 mm pupil condition.

One point might be made here; the illumination for the point images is coherent, while the illumination for the line images is incoherent. The inherent differences in the behavior of incoherent and coherent light, the most significant of which is that coherent light amplitude is linearly mapped in space, while it is the incoherent light intensity which is linearly mapped in space. However, the intensity distribution produced by a coherent uniform plane wave at the cornea is the same, except for a scaling factor, as that which would be produced by an incoherent uniform plane wave

Westheimer (12) has found that, using the method and results of Jones (6), point spread functions, when used to calculate line spread functions similar to those he measured in human eyes, are approximately 2/3 as wide between half height points as the corresponding line spread functions. Table 5 shows the corrected widths between half height points of the laser point images, (previously shown in Table 4), multiplied by 1.5, thus giving values for widths of hypothetical line spread functions derived from the point image data. The figures for Monkey 72177 (no pupil) are a little more than half the size of the measured line images of Monkey 9477, as well as those of Enroth-Cugell in the cat. The figures for Monkey 72177 with a 1 mm pupil are slightly larger than the measured line images, which are all more than twice the size of the best image obtained by Enroth-Cugell for a 1 mm pupil.

All of the figures for Monkey 10477 are from 15% to as much as 85% larger than the widths of the measured line images for Monkey 92077, the poorer of the two line image experiments.

The images for Monkey 92077 have already been suggested to be out of focus. The eye of Monkey 10477 may possibly have been of poorer quality than the other three.

The state of the eye, which may change during the course of an experiment, is possibly a significant factor in the quality of the image data obtained. Improvement was noted in the quality of images when the contact lens was removed, rinsed and replaced in the eye following the instilling of artificial tears. The condition of the cornea and fundus was difficult to judge, unless

TABLE 5

Widths between Half Height Points of Equivalent Line Images Calculated from Widths of Point Images

Monkey	Pupil	NM	Corrected Width Point Image	Equivalent Width Line Image
72177	None	630	1.98	2.97
	4 mm	630	1.8	2.7
	3 mm	630	1.98	2.97
	1 mm	630	3.5	5.25
	None	590	2.88	4.32
	None	560	2.52	3.78
	1 mm	514.5	3.91	5.87
	1 mm	488	3.72	5.58
	1 mm	455.5	5.04	7.56
10477	None	514.5	4.51	6.77
	4 mm	514.5	2.79	4.19
	3 mm	514.5	3.72	5.58
	2 mm	514.5	2.97	4.46
	1 mm	514.5	2.7	4.05
	None	488	3.28	4.92
	4 mm	488	2.88	4.32
	3 mm	488	2.88	4.32
	2 mm	488	2.7	4.05
	1 mm	488	1.8	2.7
	None	455.5	3.06	4.59

4 mm	455.5	4.09	6.14
3 mm	455.5	2.79	4.19
2 mm	455.5	3.91	5.87
1 mm	455.5	3.91	5.87

something was drastically wrong. The appearance of the fundus in the fundus camera could be misleading for two reasons; (1) the focal plane of the image should be near the probe tip, which is in front of the retinal layers and blood vessels, and (2) the eye of the observer can correct for errors in focus of either the animal's eye or the fundus camera, and it can also correct for some spherical aberration.

The eye of the animal, while in vivo, is definitely out of its "natural state", the state in which there is a proper amount of tearing, blinking, and psychophysical controls to aid the animal in forming an image.

Very small images are noted by Westheimer (11) in which the aerial images reflected off human fundi were scanned. In this work, each subject fixed his eye at a target point behind the stimulus, rather than on the stimulus itself. The best point images were calculated by Gubisch (5) from measured modulation transfer function derived from subjective (human) perception of variable spatial frequency gratings (2). In this latter work, the characteristics of the optical system were separated from the total system. Nevertheless, the focus and other fine adjustment of the optical system should have been optimum or nearly so, due to the closed loop control of the overall visual system. Their data are near the diffraction limit for all pupil sizes employed. Line images, reflected off human fundi, were also measured by Campbell and Gubisch; their results were comparable to line images derived from the psychophysical measurements.

The visual acuity of the rhesus monkeys used in the experiments, although not individually determined, has been measured

for other monkeys of the same species using a system involving the perception of the position of the gaps in Landolt C-rings (4); a task not unlike the perception of gaps of letters in the standard eye chart for humans. The acuity of the monkeys tested was 20/20 or better. The quality of a "normal" monkey eye should be very comparable to that of a "normal" human eye.

The contact lenses in corrective powers were specially made to fit the eye of an "average" monkey. This does not insure a perfect fit on each monkey used, of course, and poor lens fit may have contributed to the problem of obtaining small images.

The best point image data obtained in this work was for Monkey 72177 with all pupil conditions at 630 nm; with no pupil at 590 nm and 560 nm, and with a 1mm pupil at 488, 455.5, and 514.4 nm. (See Table 4) The width (between half-height points) of even the best of these points (3 mm pupil, 630 nm) is nearly 4 times larger than the diffraction limited spot for the same condition (See Table 6).

Another possible problem in the measurement of these images is the error introduced by rotating the eye; i.e., the rotation of the cornea as well as the retina and the resulting spread of the measured image.

To investigate this problem, a scan was made of the image of the line source produced by a 2 cm focal lens with a nominal 3 mm pupil. The lens was placed in the same position on the stereotax as an eye would be. The scan was made rotationally, just as in the eye, and also was made by translating the probe with respect to the image in 1.11 micron steps via an hydraulic

TABLE 6

Diffraction Limited Spot Diameters

Pupil Diameter	NM	Angular Width between First Zeroes (arc min)	Angular Width between Half-Height Points (arc min)
4 mm	455.5	0.96	0.4
3 mm	455.5	1.26	0.54
2 mm	455.5	1.9	0.8
1 mm	455.5	3.8	1.6
4 mm	488.0	1.04	0.44
3 mm	488.0	1.36	0.56
2 mm	488.0	2.04	0.86
1 mm	488.0	4.10	0.90
4 mm	514.5	1.06	0.46
3 mm	514.5	1.44	0.60
2 mm	514.5	2.16	0.90
1 mm	514.5	4.30	1.80
4 mm	560.0	1.16	0.46
3 mm	560.0	1.54	0.64
2 mm	560.0	2.30	0.96
1 mm	560.0	4.6	1.92
4 mm	590.0	1.24	0.54
3 mm	590.0	1.64	0.70
2 mm	590.0	2.46	1.04
1 mm	590.0	4.94	2.06
4 mm	630.0	1.32	0.55

3 mm	630.0	1.76	0.74
2 mm	630.0	2.64	1.10
1 mm	630.0	5.28	2.21

microdrive. Comparison of the two scans showed that the rotational scan was from 6 to 9% wider at half height points than the translational scan. The rotational scan apparently accounts for only a small error in the measured images.

The sizes of minimally small images limit spatial resolution in that, if two images are placed close enough together, the algebraic sum of the two profiles contains no discernible "dip" in the center, and is indistinguishable from a single image profile.

The Rayleigh limit of resolution for diffraction limited optical systems occurs when the peak of one Airy disk (point image profile) occurs at the first zero of another disk. The algebraic sum of these so-displaced functions contains a 25% "dip" in the ceter; indeed, the profiles could be moved somewhat closer together before the dip disappeared altogether.

The spot size for a 2.3 mm pupil in the human eye, at a wavelength of 555 nm, forms the basis for the 1 arc minute resolution criterion for the human eye (13); i.e., the distance from the peak to the first zero of this image profile (which is very close to an Airy disk) subtends 1 minute of arc in the eye.

The eye appears not to be performing any special "tricks" to attain this degree of resolution; Westheimer (13) has demonstrated that under certain conditions, visual acuity can be 10 times better than the diffraction limit.

Therefore, spot sizes smaller than those measured in this work must be formed on the retina under "natural" conditions for the eye.

The modulation transfer function specifies the attenuation

of spatial frequencies in the eye. A "cutoff frequency" for a diffraction limited coherent or incoherent optical system has a clear-cut meaning: the aperture(s) of the system prevent(s) high-order diffracted rays (high spatial frequencies) from appearing in the "output" of the system. Diffraction limited cutoff frequencies for several wavelengths and various pupil sizes are shown in Table 7.

In a non-diffraction limited system such as the eye, where "smearing" of spatial frequencies occurs, a definition of a cutoff frequency would have to consider the signal to noise ratio of the system. In most linear (temporal) systems such as electronic circuits, a "cutoff frequency" is defined as the frequency at which the power in the output signal is one-half of the power in the signal at "mid-band", or the frequency range in which the least amount of signal attenuation occurs.

For a "cutoff frequency" to have significance in terms of the resolution of a system, it would have to mean a frequency at or above which the information is indistinguishable from the noise of a system. Measurements of <u>contrast transmission</u> could produce finite contrast in high spatial frequencies if the overall brightness for all spatial frequencies were high enough. Discussion of a "cutoff frequency" which occurs below the diffraction limit must, it would seem, include consideration of the dicrimination capabilities of the retina receptor grid as well as higher neural processing capabilities.

"Noise" of unknown origin, in the form of discontinuities and sharp minor peaks in the measured images tends to (erroneously)

TABLE 7

Diffraction Limited Cutoff Frequencies

Pupil Diameter	NM	Cutoff Frequency Incoherent Illum. Cycles/Degree	Cutoff Frequency Coherent Illum. Cycles/Degree
4 mm	455.5	76.68	153.27
3 mm	455.5	57.48	114.95
2 mm	455.5	38.32	76.63
1 mm	455.5	19.16	38.32
4 mm	488.0	71.53	143.06
3 mm	488.0	53.65	107.29
2 mm	488.0	35.76	71.53
1 mm	488.0	71.53	143.06
4 mm	514.5	67.85	135.69
3 mm	514.5	50.88	101.77
2 mm	514.5	33.92	67.85
1 mm	514.5	16.96	33.92
4 mm	560.0	62.33	124.67
3 mm	560.0	46.75	93.5
2 mm	560.0	31.17	62.33
1 mm	560.0	15.59	31.17
4 mm	590.0	59.16	118.33
3 mm	590.0	44.37	88.75
2 mm	590.0	29.58	59.16
1 mm	590.0	14.79	29.58

4 mm	630.0	55.41	110.81
3 mm	630.0	41.56	83.11
2 mm	630.0	27.70	55.41
1 mm	630.0	13.85	27.70

contribute to the high spatial frequency content of the MTF. It would appear that information regarding spatial resolution should be derived from the widths between half height points of the line and point images. The widths measured in this work, once again, are larger than those predicted by known capabilities of the eye.

The relatively large images obtained in this work bring up the question of the possible overestimation of eye quality in the experiments of Campbell and Gubisch and Campbell and Green. The psychophysical experiment of Campbell and Green may indicate better than actual eye performance since some scattering or other degradation effects may be "cancelled out" in the process of separating the neural and optical visual system components. The physical experiment of Campbell and Gubisch, in which a line image reflected off the human fundus was measured, deals with a "double pass" of light rays through the eye. The reflection at the fundus is considered to be nearly ideal, and the eye's optics are considered perfectly reversible in their work. Any flaws in these assumptions would tend to degrade a measured image; it is hard to imagine any effect which would erroneously sharpen it. It is felt that these data are true estimates of eye performance, and the measurements made in this work indicate that the condition of the eye is poor in the experimental preparation that it is normally.

Transmission of the Ocular Media

The transmission of the ocular media values obtained for the rabbit are somewhat lower than the values of Geeraets and Berry,

while the values for the monkey are somewhat higher (See Figures 21 and 22).

Geeraets and Berry essentially measured the total transmission of the eye, including scatter. The 600 micron diameter fiber optic probe used in this work measured the direct transmission of a 200 micron $1/e^2$ diameter bean, and scattered light which lay within the probe aperture. The poorer quality rabbit eye may have scattered a significant portion of the light beyond the probe aperture, thus making the amount of light measured inside the rabbit eye lower than the amount measured by Geeraets and Beery.

The higher quality monkey eye probably scattered less light than the rabbit eye; therefore, more light was incident on the probe aperture. The quality of the monkey eye may have been better than that of the 2 cm. focal length lens used to calibrate the probe response (See Experimental Procedure section). This would make the transmission values for the monkey higher than they actually are.

The variation in the individual points could be due to a change in the imaging conditions (divergence of the beam) for each measurement; also, the amount of scattered light could have changed due to a change in the condition of the eye. Another possible source of variation would be an error in power measurement with the radiometer, either of power incident on the probe (outside the eye) or incident on the cornea (with the probe inside the eye).

The coupling of light into a fiber optic in general is different when the fiber is in air and when the fiber is in water.

The coupling is primarily influenced by the difference in refractive index at the probe interface. The fiber optic probe used in these measurements had a diffusing surface; reflections off this surface are non-specular and do not depend on the medium the probe is in. The response of this probe should be the same in water-like media as in air.

CONCLUSIONS

The results of this work lead to the following conclusions:

A fiber optic probe is a useful device for measuring the relative light intensity distribution within the eye of an anesthetized experimental animal. The minimally small images measured were larger than those measured by others or predicted by diffraction theory. Possible reasons for the relatively poor results here are (1) the lack of a proper tear layer on the cornea in the anesthetized animal; (2) disturbance of the corneal refracting surface by the contact lens, which may not have fit properly and was changed during the experiment; (3) the lack of fine focusing or micro-accomodation activity in the crystalline lens, since the ciliary muscle was paralyzed and did not function as it does in an alert animal; and (4) possible unknown factors, such as changes in intraocular pressure, affecting the condition of the eye in the anesthetized state of the animal. For these reasons, the errors introduced in measuring small images reflected off the fundus in alert human subjects are probably not due only to instrumentation and not the lack of fine focusing. Data from visual acuity tests suggest that the optical quality of alert monkeys is indeed comparable to that of humans. Nevertheless, the results obtained here should be valid for other experiments in which eye quality is measured, or the quality of the eye affects the outcome, and the experimental animal is anesthetized as in this work.

A fiber optic probe is a reasonably accurate device for measuring the transmission of the ocular media in experimental animals. Laser sources were used in this work, providing a limited number of wavelengths. The increased sensitivity of a broadband photomultiplier detector would allow a tungsten or xenon source with a monochromator to be used, giving a more complete spectral response curve.

BIBLIOGRAPHY

1. Cain, C.P. and Welch, A.J., "Dynamic Spatio-Temporal Temperature Measurements in Laser Irradiated Rabbit Eyes," Technical Report 138, Electronics Research Center, The University of Texas at Austin, September, 1972.

2. Campbell, F. W., "The Human Eye as an Optical Filter," Proceedings of the IEEE, Vol. 56, p. 1009, June, 1968.

3. Geeraets, W.J. and Berry, E.R., "Ocular Specular Characteristics as Related to Hazards from Lasers and Other Light Sources," American Journal of Ophthalmology, Vol. 66, p. 15, July, 1968.

4. Graham, Ernest S., Farrer, Donald N., Crook, Guy H. II, Garcia, Paul V., "A Self-Adjustment Procedure for Measuring the Visual Acuity of Rhesus Monkeys," Behavior Research Methods and Instrumentation, Vol. 2, p. 301, 1970.

5. Gubisch, R.W., "Optical Performance of the Human Eye," Journal of the Optical Society of America, Vol. 57, p. 407, March, 1967.

6. Jones, R. Clark, Photo. Sci. Eng., 2, 198 (1958).

7. Kidwell, T.P., "Transmission of the Ocular Media in Argon Laser Irradiated Rabbit Eyes," Investigative Ophthalmology, Vol. 15, pp. 668-671, August, 1976.

8. Priebe, L.A., Cain, C.P. and Welch, A.J., "Temperature Rise Required for Production of Minimal Lesion in the Macaca Mulatta Retina," American Journal of Ophthalmology, Vol. 79, No. 3, p. 405, 1975.

9. Robson, J.G., and Enroth-Cugell, C., "Light Distribution in the Cat's Retinal Image," submitted to Vision Research.

10. Siegman, A.E., An Introduction to Lasers and Masers, Chapter 8, McGraw-Hill, 1971.

11. Westheimer, G. and Campbell, F.W., "Light Distribution in the Image Formed by the living Human Eye," Journal of the Optical Society of America, Vol. 52, p. 879, November, 1954.

12. Westheimer, G., "Optical and Motor Factors in the Formation of the Retinal Image, "Journal of the Optical Society of America, Vol. 53, p. 86, January, 1963.

13. Westheimer, Gerald, "Diffraction Theory and Visual Hyperacuity," American Journal of Optomertry and Physiological Optics, Vol. 53, p. 362, July, 1976.

SECURITY CLASSIFICATION OF THIS PAGE (When Data Entered)

REPORT DOCUMENTATION PAGE

READ INSTRUCTIONS BEFORE COMPLETING FORM

1. REPORT NUMBER: AFOSR-TR-79-0672	2. GOVT ACCESSION NO.
3. RECIPIENT'S CATALOG NUMBER	
4. TITLE (and Subtitle): MEASUREMENTS IN THE LASER IRRADIATED EYE.	5. TYPE OF REPORT & PERIOD COVERED: FINAL 01 April 1977-31 March 1978
	6. PERFORMING ORG. REPORT NUMBER
7. AUTHOR(s): Ashley J. Welch & Larry D. Forster	8. CONTRACT OR GRANT NUMBER(s): AFOSR-77-3314
9. PERFORMING ORGANIZATION NAME AND ADDRESS: University of Texas at Austin, Bio-Medical Engineering Laboratory, Austin, Texas 78712	10. PROGRAM ELEMENT, PROJECT, TASK AREA & WORK UNIT NUMBERS: 61102F 2312 2312A5
11. CONTROLLING OFFICE NAME AND ADDRESS: Air Force Office of Scientific Research (NL), Bolling AFB DC 20332	12. REPORT DATE: 15 Nov 1978
	13. NUMBER OF PAGES: 68
14. MONITORING AGENCY NAME & ADDRESS(if different from Controlling Office): Final rept. 1 Apr 77 - 31 Mar 78,	15. SECURITY CLASS. (of this report): Unclassified
	15a. DECLASSIFICATION/DOWNGRADING SCHEDULE

16. DISTRIBUTION STATEMENT (of this Report)

Approved for public release; distribution unlimited.

17. DISTRIBUTION STATEMENT (of the abstract entered in Block 20, if different from Report)

18. SUPPLEMENTARY NOTES

19. KEY WORDS (Continue on reverse side if necessary and identify by block number)

Eye, Laser, Micro Sensors

20. ABSTRACT (Continue on reverse side if necessary and identify by block number) The work described in this report involves the fabrication and use of a small fiber optic probe to measure (1) the transmission of the ocular media which is the ratio of the total light intensity reaching the retina to the total light intensity incident on the cornea, and (2) the cross-sectional intensity profile of a niminally small image. Information concering the resolution of the eye is derived from the small image measurements.

409 319

DD FORM 1 JAN 73 1473 EDITION OF 1 NOV 65 IS OBSOLETE

UNCLASSIFIED

JOB

Critical parameters in the study of damage mechanisms in the eye are the amount of light reaching the retinal tissues as a function of wavelength, and the size and shape of the relative light intensity distribution on the retina.

Measurements of these quantities have been reported in the literature. Most of the measurements of the transmission of the ocular media were made on excised eyes and most of the measurements of minimal retinal images were made either on excised eyes, or were made indirectly on intact eyes by a fundus reflective or psychophysical technique. In this research direct, in vivo measurements of these two quantities were made in the rhesus monkey eye.

The transmission of the ocular media, measured on a limited number of animals, compares well with some of the best previously reported data. The transmission was measured via a 600 micron diameter fiber optic probe which collected all the light from a 200 micron diameter irrading laser beam. Three lasers, providing seven wavelengths, were employed.

The minimal images measured in the monkey eye were larger than values reported from subjective acuity tests or by diffraction theory. Some of this poor quality could be attributed to experimental error, but perhaps the most significant factor affecting eye quality was the fact that the neural controls for blinking, tearing, and microaccomodation, which aid the eye in forming a retinal image, were inactive in the anesthetized animal. If eye quality in the experimental preparation is indeed poor, other experiments involving fine visual detail would be similarly affected.